UNIVERSITY OF WISCONSIN-LA CROSSE

Graduate Studies

IDENTIFICATION OF A NOVEL LATE DOMAIN IN HUMAN PARAINFLUENZA VIRUS TYPE 3 MATRIX PROTEIN

A Chapter Style Thesis Submitted in Partial Fulfillment of the
Requirements for the Degree of Master of Science

Christine E. Hulseberg

College of Science and Health
Biology/Clinical Microbiology Concentration

December, 2010

IDENTIFICATION OF A NOVEL LATE DOMAIN IN HUMAN

PARAINFLUENZA VIRUS TYPE 3 MATRIX PROTEIN

By Christine E. Hulseberg

We recommend acceptance of this thesis in partial fulfillment of the candidate's requirements for the degree of Master of Science in Clinical Microbiology.

The candidate has completed the oral defense of the thesis.

Michael Hoffman — 12-16-10

Michael Hoffman, Ph.D.
Thesis Committee Chairperson

Date

Scott Cooper — 12-16-10

Scott Cooper, Ph.D.
Thesis Committee Member

Date

[signature] — 12-16-10

Anton Sanderfoot, Ph.D.
Thesis Committee Member

Date

[signature] — 12/16/10

Todd Weaver, Ph.D.
Thesis Committee Member

Date

Thesis accepted

Vijendra K. Agarwal — 2/23/11

Vijendra K. Agarwal, Ph.D.
Associate Vice Chancellor for Academic Affairs

Date

ABSTRACT

Hulseberg, C.E. Identification of a novel late domain in human parainfluenza virus type 3 matrix protein. MS in Biology: Clinical Microbiology Concentration, December 2010, 68 pp. (M.A. Hoffman).

Human parainfluenza virus type 3 (HPIV3) is a major cause of bronchiolitis and pneumonia in infants under 6 months of age. Like other enveloped RNA viruses, HPIV3 encodes a matrix (M) protein involved in the final assembly and budding steps of the viral life cycle. Illustrating the important role of M protein is its ability to induce its own budding from cells in the form of enveloped virus-like particles (VLPs). For related viruses, the feature of viral M proteins that allows this independent budding to occur is a critical amino acid sequence, called a late (L) domain, which interacts with the host cell vesicle-forming machinery. To identify the HPIV3 L domains, we selected four HPIV3 M protein sequences (PPKH, YLDV, KPEL, and YPNI) based on their sequence similarity to established L domains and made alanine-substitution mutants of each potential L domain sequence. When these mutant M proteins were expressed in cells, we found that disrupting the YLDV sequence caused a severe budding defect. To confirm these results, we then inserted these sequences into poorly budding L domain-deficient mutants of the Ebola virus matrix protein. Consistent with our previous findings, the YLDV-containing VP40-ΔN13 mutant was able to restore budding efficiency to levels on par with wild-type VP40. These findings provide strong evidence to support the likelihood that the YLDV sequence of HPIV3 M protein functions as an L domain.

ACKNOWLEDGEMENTS

The person to whom I owe the greatest debt of gratitude is my advisor, Dr. Michael Hoffman. Without his mentorship, patience, and good humor throughout my prolonged stay here at UW-La Crosse I would have long ago given up. The members of my thesis committee also deserve much appreciation for their valuable insight and advice during my research. They are: Drs. Scott Cooper, David Howard, Todd Weaver, Anton Sanderfoot, and Jeffrey Sartin, M.D. Among my peers here, I owe especial thanks to Marisa Barbknecht and Jill Gander, whose knowledge and guidance were of tremendous help when I first began my research. My other labmates and friends, Megan Bracken, Kelly Rock, and Aliberkys Lopez, were incredibly cooperative, hardworking, fun, and supportive. LeRoy Bierfreund, Steve Cash, Brandon Reuter, and Peter Ladell were very generous with their time and helpful in offering advice. These individuals all made coming to lab a joy. I am grateful for the financial support from the UW-La Crosse Research, Service, Education, and Leadership (RSEL) grants for graduate research and travel as well as the UW-La Crosse Microbiology Department for providing me with an assistantship during my time here. Finally, I would like to thank Don, Sandy, Paul, and Orathai – the greatest family in the world – for their constant encouragement and support.

TABLE OF CONTENTS

PAGE

LIST OF FIGURES

CHAPTER I

INTRODUCTION

Human parainfluenza virus 3 (HPIV3) is a common cause of minor colds and more serious lower respiratory tract infections (LRIs), particularly bronchiolitis and pneumonia. Young children, the elderly, and immunocompromised individuals are especially susceptible to infection, which can occur repeatedly throughout life. Each year, approximately 1 million people in the United States require medical attention because of an HPIV3-related illness. Between 18,000 and 29,000 of these cases are severe enough to warrant hospitalization, although mortality is quite low in the US and other developed countries. In developing countries, however, young children are at considerable risk for HPIV-induced death (26). Globally, viral LRIs claim millions of lives and are particularly threatening for newborns and children with underlying cardiac, pulmonary, and immunodeficiency disease (46, 83). In fact, LRIs – largely caused by the parainfluenza, influenza, and respiratory syncytial viruses – remain the leading cause of death due to infectious disease worldwide (39, 78).

Typical upper respiratory HPIV3 infections are brief and largely mitigated by the host innate immune response. Acquired immunity following acute infection is often short-lived, making recurrent infections common – although less severe – throughout life. Infants are protected from infection by maternal antibodies for the first four months of

life, but after the titers of maternal antibodies decline, the rate of HPIV3 infection steadily climbs until around 18 months of age. HPIV3 infections are so common during early childhood that by the age of three nearly all children demonstrate some serologic memory when presented with HPIV3 antigenic challenge (27).

Infected adults often are asymptomatic or have mild disease because of the rapid and efficient clearance by the immune system. As the competence of immune and respiratory function diminishes with advanced age, elderly individuals become increasingly susceptible to more severe HPIV3 infections. The extent of susceptibility among the elderly population has been highlighted by prospective studies in nursing homes, which found that HPIV infections were responsible for 4%–14% of lower respiratory illnesses (13). Of the four serotypes of human parainfluenza viruses (HPIV1-HPIV4), HPIV3 is the most common and the most virulent (48).

Since seasonal outbreaks of HPIV3 infections are most frequent during the spring and summer months, diagnosis of HPIV3 infection is generally supported if the timing of a respiratory illness occurs during warmer seasons. Still, diagnosis can be confirmed by conventional laboratory methods if the severity of infection warrants a definitive diagnosis (14). However, since a number of infectious agents, both viral and bacterial, may cause respiratory symptoms similar to HPIV3 infection, treatment options are generally kept nonspecific and supportive in cases of less serious infection. Even in instances where a definitive diagnosis of HPIV3 infection has been made, there are no specific treatments for HPIV infections, unlike influenza and respiratory syncytial virus.

Although some research has been devoted to developing antiviral therapies for severe HPIV3 infections (46, 65, 73), most emphasis is directed toward producing a

viable HPIV3 vaccine. The humoral response to HPIV3 infections is mostly conferred by IgG in the serum and IgA in the mucosa against viral surface proteins, but the cell-mediated response plays an especially critical role in controlling the extent of infection by quickly clearing the virus after exposure (12, 17, 47). Hence, much of the focus in vaccine development has been on the development of an immunogenic and protective live attenuated virus vaccine that can induce both the humoral and cellular arms of the immune system. Several attempts have been made to develop live attenuated HPIV3 vaccines, one of which is a temperature-sensitive virus currently in Phase II/III clinical trials (12, 39, 41). To date, however, neither an FDA-approved antiviral drug nor vaccine for HPIV3 is available in the US.

Characteristics of HPIV3

HPIV3 Classification

HPIV3 is grouped in a large order of enveloped, non-segmented, negative-sense RNA viruses called the *Mononegavirales.* This order contains many clinically relevant viruses, including the Ebola and Marburg viruses (EbV and MARV) in the *Filoviridae* family, and rabies virus (RV), in the *Rhadboviridae* family. The parainfluenza viruses belong to a third family within *Mononegavirales*, the *Paramyxoviridae* (Fig. 1A). Among the many clinically important viruses in this diverse family are: RSV, the leading cause of bronchiolitis in children; measles virus, which caused 345,000 deaths worldwide in 2005 (1, 78, 82); Nipah virus (NiV), an emergent biosafety level 4 virus (8); and Newcastle disease virus (NDV), a highly contagious avian virus (Fig. 1B) (26). HPIV3, along with HPIV1, a bovine-specific PIV3 (BPIV3), and Sendai virus (SeV), are classified within the genus *Respirovirus,* one of the eight genera of the *Paramyxoviridae*.

Order *Mononegavirales*

A

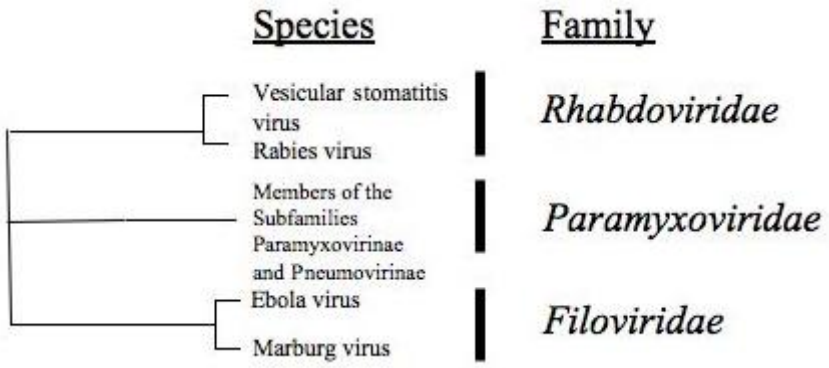

B

Family *Paramyxoviridae*

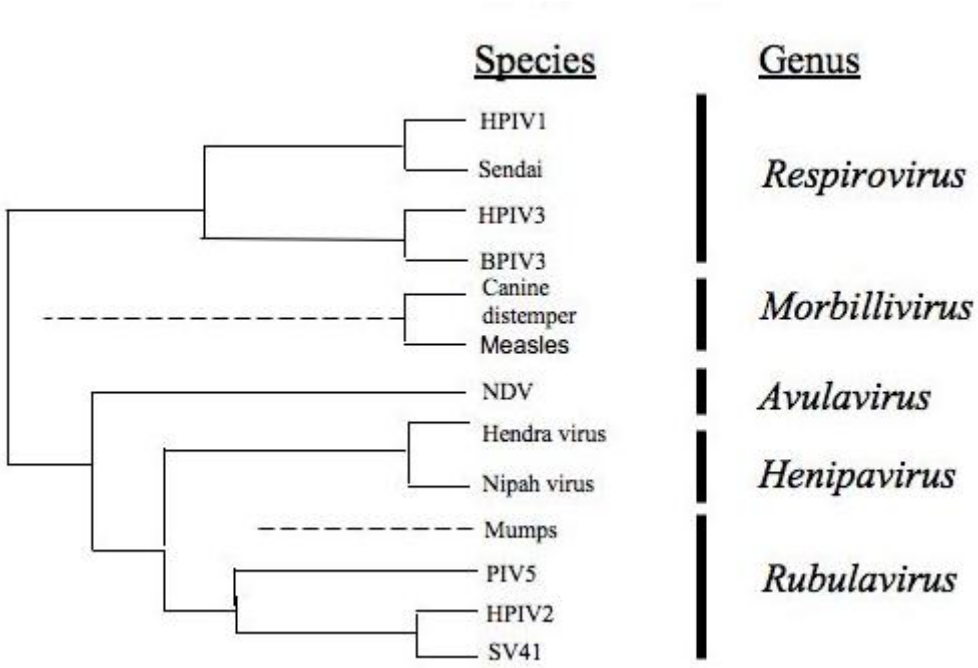

Fig. 1. Phylogenetic tree illustrating relationships of clinically important viruses. A. Members of the order *Mononegavirales*. B. Five of the eight genera in the family *Paramyxoviridae*. RSV is not shown because, although it is a member of the *Paramyxoviridae*, it is classified in a separate subfamily, the *Paramyxovirinae*. Divergences are not to scale. Dotted lines indicate degrees of different protein sequence relatedness that make exact classification equivocal.

HPIV3 Structure

HPIV3 virus particles are pleomorphic in shape, range in diameter from 150 to 200 nm, and contain a 15,462 nucleotide genome which encodes six structural proteins (67) (Fig. 2B). The 71 kDa hemagglutinin-neuraminidase (HN) and 65 kDa fusion proteins (F) are both lipid envelope glycoproteins which form spikes 8-12 nm in length that can be seen protruding out from the surface of virus particles in electron micrographs. The 68 kDa nucleocapsid (N) protein coats the entire length of the viral genome. This N-RNA complex forms a stable, flexible coil with the acidic carboxy terminus of the N protein extending away from the RNA while the more basic amino terminus associates with other N subunits and the RNA genome. Both the 90 kDa phosphoprotein (P) and the 255 kDa large protein (L) associate with the acidic carboxy terminus of the N protein to form the core of the virus particle, which is referred to as the ribonucleoprotein (RNP) complex. The carboxy domain of P protein binds the L protein. The highly basic 40 kDa matrix (M) protein, the most abundant virus particle protein, lines the viral envelope surrounding the nucleocapsid and interacts with the short inward-facing carboxy-terminal tails of the F and HN transmembrane proteins (Fig. 2A).

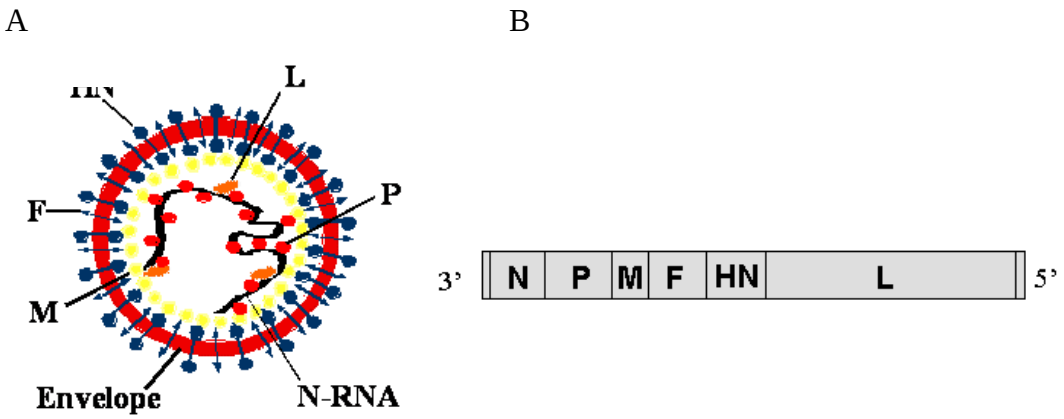

Fig. 2. Schematic representation of the structure of HPIV3. A. The M protein lines the interior of the virus particle. B. The organization of the HPIV3 genome.

HPIV3 Life Cycle

Attachment and entry. The life cycle of *Mononegaviruses* begins when the viral particle comes into contact with epithelial cells lining the respiratory tract (Fig. 3). The HN protein attaches to the sialic acid-containing surface receptors of the host cell (29). After attachment to cellular receptors, the F protein interacts with the cellular lipid bilayer and triggers a fusion between the viral membrane and the cell membrane. When this membrane fusion occurs, the RNP complex is released into the cytoplasm of the host cell.

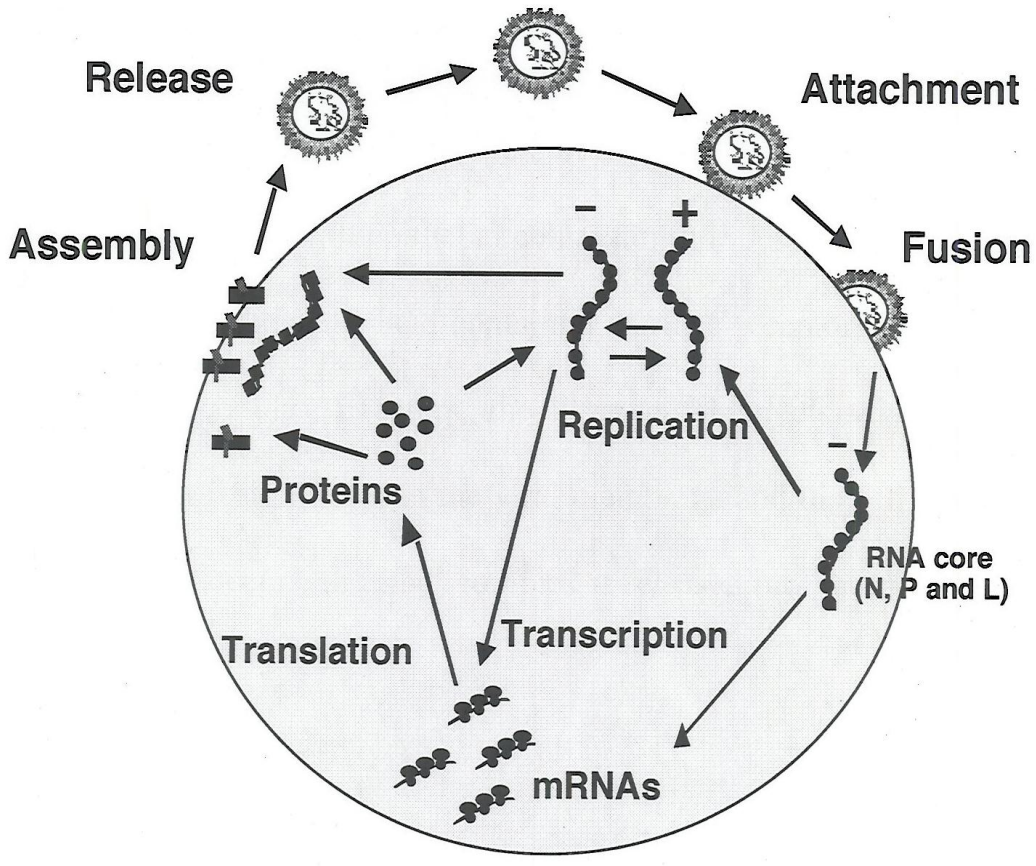

Fig 3. Life cycle of HPIV3 in human cell host from attachment to release.

Transcription, protein synthesis and genome replication. Once the RNP complex enters the host cytoplasm, the synthesis of new viral proteins and additional copies of the viral genome begin. Because replication cannot be completed without *de novo* synthesis of viral proteins, the first biosynthetic steps are transcription and translation (27, 60). During transcription, the P and L proteins form the viral polymerase complex and sequentially transcribe each gene via a start-stop mechanism while traveling 3' to 5' on the template. The 3' end of each transcript is polyadenylated while the 5' ends are capped and methylated by the L protein (51). The mRNAs are then translated by cellular ribosomes, beginning a gradual accumulation of viral proteins in the cytoplasm.

Following early production of viral proteins, newly synthesized polymerase complexes begin to replicate the viral genome. Replication begins with the synthesis of (+) sense antigenomic RNA from the (-) sense genome. This (+) sense template is then used to generate additional copies of the (-) sense genome. Throughout genome replication and transcription, N proteins remain bound to the genome and antigenome.

Assembly and release. As genome replication continues, newly synthesized viral proteins localize to different positions in the cell. The RNP complexes remain in the cytoplasm while the HN and F membrane proteins are routed to the plasma membrane via the endoplasmic reticulum and the secretory pathway (2, 22, 27).

Once progeny genomes are synthesized, assembly of viral components must occur before new virus particles can be released from the host cell. Clusters of all the components needed in mature virus particles – present in stoichiometrically proportional levels – begin to accumulate at the plasma membrane (2). M protein, which acts a bridge

between the HN and F glycoproteins and the RNP complex, is critical in coordinating the assembly of viral components at the plasma membrane (15, 40).

Once viral protein clusters have organized at the budding site on the plasma membrane, the lipid bilayer is pushed outward until membrane fission occurs, in a manner analogous to the cellular process of vesicle formation. The neuraminic acid activity of HN protein cleaves sialic acid residues from the exterior of the cell and viral envelope, which would otherwise result in the formation of ineffectual aggregates of nascent virus particles (29). Once the virion is released from the cell surface, its life cycle is complete and the mature virus particle may find a new cell to infect.

The Role of Matrix Protein in Release

The viral matrix protein orchestrates both the localization of viral proteins during assembly (9) as well as the release of virus particles (6). The importance of matrix protein in the budding process has been demonstrated by assays involving the introduction of plasmid-encoded viral matrix genes into mammalian cell lines. The M protein synthesized in transfected cells is detected not only in cells but also in the media, in the form of vesicle-bound virus-like particles (VLPs) that have budded from the host cell as occurs in natural infections. The remarkable ability of matrix proteins to bud on their own is a property unique among viral proteins and underscores the crucial role of M proteins as the mediator of virus particle release. Such budding assays can provide valuable insight regarding the key, conserved role for matrix protein in the release of enveloped viruses (19, 35, 62).

VLP budding assays allow investigators to accurately quantify and compare the budding efficiency of matrix proteins in different experimental conditions. To quantify VLP production, most budding assays involve adding ^{35}S methionine to methionine-depleted cells expressing viral M protein. After the radioisotope has been incorporated into newly synthesized proteins, the supernatant is collected and the cells are lysed. To visualize M protein from VLPs in the media, the VLPs are purified from non-enveloped cellular proteins by ultracentrifugation through a sucrose cushion. Alternatively, the media can be treated with a detergent to solubilize the VLP membrane and release the M protein so that it can be immunoprecipitated with an α-M antibody. The radiolabeled M protein from the cell lysate and detergent-treated/ultracentrifuged VLPs from the media can then be separated by SDS-PAGE and visualized on a phosphorimager.

Through budding assays much has been discovered about the unique properties of M protein that enable it to bud independently from cells. Furthermore, budding assays provide an alternative to using potentially dangerous live viruses in these studies – an advantage which has been especially important in research involving highly lethal viruses such as EbV. VLP production assays avoid the use of fully infective live viruses and allow us to safely examine and manipulate individual viral components to learn about their role in assembly and/or release.

Late Domains

The mechanism behind M protein release is not well understood, but there is evidence that many M proteins lack the means to provide the biophysical force for budding. For release of enveloped viruses, a critical reliance on cellular pathways had long been suspected in the budding process because the budding of virus particles from

the plasma membrane is topologically equivalent to the budding of vesicles that occurs in some cellular protein-sorting pathways. As predicted, many enveloped viruses appear to subvert the host cell's protein sorting pathway to accomplish the final budding event of the viral life cycle.

Initial evidence that enveloped viruses rely on cellular factors to bud was provided by experiments with HIV-1. In 1991, Göttlinger et al. (21) showed that a deletion in the C-terminal region of HIV-1 Gag protein resulted in the assembly of normal virus particles, but these particles could not separate from the host cell. Electron microscopy confirmed that, although these mutants had successfully assembled in ready-to-bud vesicles, they remained tethered to the plasma membrane of the host cell by long stalks.

Mutational analysis of this C-terminal region in Gag later revealed that the short peptide motif, PTAP, was responsible for conferring budding ability in HIV-1 (28). The disruption of this late life cycle event by mutations in PTAP led to its designation as a viral "late" domain. Several years after the discovery of HIV's PTAP late (L) domain, Parent et al. (56) discovered that the L domain of the Roux sarcoma virus, another retrovirus, was interchangeable with the HIV L domain. By inserting the Roux sarcoma virus PPPY L domain sequence into the PTAP-deficient Gag protein of HIV, budding efficiency of Gag protein VLPs was completely restored (66, 80). Budding restoration was also observed when PTAP was inserted at different positions in the PTAP-deficient Gag (5). The small size, interchangeability, and positional independence of these L domains strongly suggested that L domains function as docking sites for recruiting cellular proteins.

To date, L domains have been identified in a diverse range of dozens of unrelated viruses, including two enveloped DNA viruses, at least five retroviruses, two arenaviruses, influenza, and all three viral families within the *Mononegavirales* (5). Despite the diversity represented by these viruses, the L domains identified thus far seem to be restricted to several motifs: PT/SAP, PPxY, YxxL, and FPIV/FPVI. For each of these motifs (except the lattermost), a specific cellular binding partner has been identified.

The Vacuolar Protein Sorting Pathway

As discussed, many viral matrix proteins are widely believed to lack the ability to independently provide the driving force needed to bud. The primary role of viral matrix proteins in the release process is therefore attributed to L domain-mediated interactions with the host cell's vesicle-forming machinery. This section will discuss how these cellular pathways function and how viruses are thought to take advantage of them to escape from the host cell.

Cells regulate surface transmembrane protein expression by endocytosing them and either recycling them to the surface or delivering them to lysosomes for degradation (3). The removal and trafficking of cellular transmembrane proteins is managed by the vacuolar protein sorting (VPS) pathway, which, in addition to fulfilling several other major functions, sorts transmembrane proteins in endosomes.

Early endosomes contain transmembrane proteins arriving from the cell surface and transmembrane proteins transiting to and from the trans-Golgi network (TGN). Some of these transmembrane proteins from the cell surface, such as nutrient receptors, are recycled to cell surface. Others, such as activated growth factor receptors, cytokine

receptors, and misfolded proteins, are transported to the lysosome for degradation. Single unit ubiquitin tags on these transmembrane proteins serve as routing slips that ensure these transmembrane proteins are degraded instead of recycled.

Ubiquitinated transmembrane proteins destined for degradation are internalized within endosomes by a series of protein complexes called endosomal sorting complexes required for transport (ESCRTs-0, -I, -II, and -III). ESCRT proteins process vesicles into the interior of the endosome, maturing the endosome into a multivesicular body (MVB). When the ESCRTs have finished processing the transmembrane proteins into vesicles within the lumen of a mature MVB, the ESCRT proteins are recycled to another early endosome to begin the process anew. The MVB then fuses with the lysosome where the transmembrane protein cargo is degraded by lysosomal proteases.

Viral M proteins are thought to seize ESCRT proteins at the surface of early endosomes and sequester them to the viral budding site at the plasma membrane (Fig. 4). Once at the plasma membrane, ESCRTs then lend their normal vesicle formation activity to facilitating the release of virus particles. The specific functions of ESCRT proteins in vesicle formation make them logical targets for budding viruses and will be described here in some detail.

First, ESCRTs recognize ubiquitinated proteins and mediate their entry into endosomes (59). Viruses with a PPxY L domain, like several retroviruses, rhabdoviruses, arenaviruses, and filoviruses, interact with cellular ubiquitin ligases. These ligases covalently add ubiquitin to the viral matrix proteins and are thought to serve as an access point for PPxY -containing M proteins to hijack the ESCRT machinery (38).

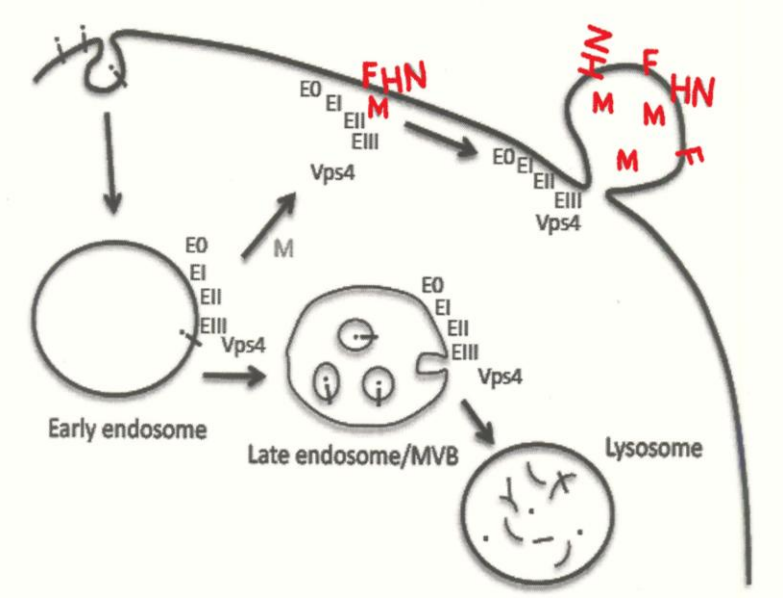

Fig. 4. Model of VPS pathway utilization by viral matrix protein (viral proteins in red). The ESCRT complexes are sequestered away from the endosome to the plasma membrane via interactions with the M protein. Once at the budding site, ESCRTs then facilitate budding.

ESCRTs are also responsible for catalyzing the curvature in the endosomal membrane, just as budding virus particles deform the plasma membrane as they push outward, away from the cytoplasm. Although the specific role of ESCRTs in the membrane deformation process is poorly understood, experimental evidence suggests that ESCRT-I and III proteins are involved in causing the curvature (4, 54). The fact that PT/SAP- and YxxL-containing M proteins interact with the ESCRT-I proteins, Tsg101 and Alix, respectively, suggests that these ESCRTs contribute to the membrane curvature at the viral budding site.

Lastly, VPS4, which interacts with ESCRT-III complex, triggers the final abscission that occurs before the vesicle is released into the lumen of the endosome. The hydrolysis of ATP by VPS4 provides the energy input to remove the ESCRT III complex from the

endosomal membrane, which causes a contraction of the membrane around the particle and, ultimately, membrane abscission (54). This final "pinching off" of inchoate virus particles must also occur before they can be released from the plasma membrane into the extracellular milieu (79). The involvement of VPS4 in M protein release is thought to be of such importance that assaying the effects of a dominant negative (DN) form of VPS4 on viral release is considered the gold standard in determining whether a virus utilizes the ESCRT machinery (6).

MVB Pathway-Mediated Virus Particle Release

Many budding viruses that derive their envelope from the host cell membrane are thought to recruit the ESCRT machinery to the plasma membrane to facilitate their release. The three major L domain motifs identified to date usurp the ESCRT machinery by binding a corresponding ESCRT protein (PPxY:Nedd4 ubiqitin ligase, YxxL:Alix/AIP1, and PT/SAP:Tsg101). This single interaction (or multiple interactions in the case of viruses with two L domains, such as EbV and HIV-1) also brings the other components of the ESCRT machinery to the membrane due to protein-protein interactions among the ESCRT complexes to initiate budding (49).

The requirement for ubiquitin in enveloped virus release is less firmly established and seems especially flexible with the retroviruses (56, 86). However, reduced budding of several mononegaviruses from cells under ubiquitin-limiting conditions has been observed. The rhabdoviruses vesicular stomatitis virus (VSV) and RV are drastically impaired in budding efficiently from cells treated with ubiquitin-depleting compounds, which results in a decrease in titer to 10% - 20% relative to the titer released from untreated cells (23, 25). Depleting Nedd4 ubiquitin ligase via siRNA caused a fivefold

decrease in the release of the matrix protein of MARV (72, 74). Titers of the paramyxoviruses PIV5 and SeV are also significantly reduced under ubiquitin-limiting cellular conditions: treatment with the proteasome inhibitor drug, MG132, resulted in the reduction of PIV5 particle release to just 23% of WT and, in SeV infections, virus particle release was stopped all together after cells received MG132 treatment (61, 77).

Regardless of which viral L domain-mediated cellular interaction is adapted to recruit MVB pathway machinery to the budding site, viruses that interact with ESCRT proteins are thought to require VPS4 to separate from the cell membrane. As described before, VPS4 is the last major player of ESCRT-mediated vesicle formation, and, accordingly, functional VPS4 is a requirement for MVB-dependent viruses to completely pinch off from the plasma membrane. To confirm the requirement for VPS4 in virus particle release, cells are usually either treated with siRNAs for VPS4 or transfected with plasmids encoding a DN VPS4 mutant (75). Electron micrographs of virus-infected cells lacking functional VPS4 reveal long stalks of virions tethered to the cell surface because they cannot completely pinch off from the membrane (18, 21).

Many viruses within the *Mononegavirales* have been shown to be dependent on VPS4 for efficient release. The budding efficiency of the EbV virions is reduced 10-fold in infected cells expressing DN VPS4 (44). Dependence on VPS4 in VSV was shown by infecting DN VPS4-expressing cells and observing an ~ 18-fold decrease in budding (23, 69). Parainfluenza virus type 5 (PIV5, previously known as SV5) particle budding is also inhibited in the absence of functional VPS4 (64). Unfortunately, SeV's reliance on VPS4 is currently unresolved, as Gosselin-Grenet et al. found no dependence on VPS4 for SeV particle release (using transient transfections to express DN VPS4) while Irie et al. found

a significant decrease in SeV M VLP release from cells overexpressing DN VPS4 (20, 35). In a later paper, however, SeV M VLP production was insensitive to DN VPS4 when SeV C protein was also expressed (34). They proposed that the two proteins have separate, complementary functions in SeV release: M protein provides the driving force for budding (and, hence, is sensitive to DN VPS4 when expressed alone) and C protein increases budding efficiency by interacting with Alix.

In summary, viral L domains appear to function by mimicking recruitment events that are normally mediated by ESCRT proteins in the MVB pathway. The convergent exploitation of MVB materials and machinery among the mononegaviruses emphasizes the importance of complex viral interactions with cellular proteins during the life cycle of these enveloped viruses.

The following section will discuss known L domain interactions with cellular ESCRT proteins. Because HPIV3 is a mononegavirus, the discussion will be limited to the filoviruses, rhabdoviruses, and paramyxoviruses.

Filoviruses. Both EbV and MARV possess bonafide L domains with the PPxY motif near the amino terminus of their matrix proteins: $_{10}$PPEY$_{13}$ in EbV and $_{16}$PPPY$_{19}$ in MARV. The matrix protein of EbV, called VP40, also has a second, overlapping PTAP L domain ($_{7}$PTAPPEY$_{13}$) which is absent in MARV VP40 and has been shown to have its own separate cellular binding partner. DN VPS4 caused a 10-fold reduction in the release of infectious EbV virions (45).

The $_{7}$PTAP$_{10}$ L domain is critical for the efficient release of EbV VP40 (44, 50, 76). Mutating the first proline to leucine caused a substantial defect in VP40 release (50). Fluorescent microscopy has also shown that this 7-LTAP mutant failed to redistribute the

cellular binding partner of $_{7}$PTAP$_{10}$, Tsg101, away from endosomes in the cytoplasm to the budding site at the plasma membrane (70). Furthermore, Tsg101 is incorporated in VP40 VLPs (it is detected in western blots of VP40 VLPs) but is not incorporated into VLPs particles made using VP40 containing a P7A mutation (45).

Demonstrating the functional importance of the second overlapping L domain in EbV VP40 ($_{10}$PPEY$_{13}$), a substitution of the fourth amino acid from tyrosine to alanine caused a 75% reduction in VP40 release relative to VP40-WT (24). In addition to inhibiting efficient VP40 release, the 10-PPEA mutation also resulted in cellular ubiquitin ligases not ubiquitinating VP40. Western blotting confirmed that the 10-PPEA mutation blocked the interaction between VP40 and ubiquitin ligase (24).

There is also evidence that EbV has additional elements outside of VP40 that contribute to efficient release. It has been shown that co-expression of EbV glycoprotein (GP) and NP significantly enhance VLP release efficiency, although the mechanism behind this enhanced release has not been fully characterized (45).

MARV also relies on a PPxY L domain ($_{16}$PPPY$_{19}$) for VP40 release. The mutagenesis of $_{16}$PPPY$_{19}$ to 16-PPPA reduced VLP release to just 30% of WT release (74). VLP release is also dependent on the cellular ubiquitin ligase Nedd4, which binds the domain $_{16}$PPPY$_{19}$ of MARV VP40. Depletion of Nedd4 resulted in a 5-fold decrease in VP40 release (72). In addition to being detected in MARV VP40 VLPs, glutathione S-transferase (GST) pull-down assays have confirmed a direct interaction between MARV VP40 and Nedd4 (72, 74).

Like EbV, MARV VP40 release is enhanced when co-expressed with an additional viral protein, in this case the NP protein. Urata et al. recently discovered that, in addition

to the $_{16}$PPPY$_{19}$ L domain in VP40, MARV encodes a second functional PSAP L domain on the NP protein. The PSAP motif of NP was shown to recruit Tsg101 to the budding site (11, 72).

Rhabdoviruses. As with the filoviruses, both RV and VSV possess amino terminus PPxY L domains (25). VSV M protein also has a PSAP motif ($_{37}$PSAP$_{40}$) but it does not appear to be a functional L domain (30).

The L domain of VSV was originally identified after observing a restoration of budding efficiency in an L domain-deficient mutant of the retrovirus Rous sarcoma virus that had been augmented with the first 74 residues from the amino terminus of VSV M (10). Alanine substitutions of a $_{24}$PPPY$_{27}$ sequence were found to reduce M protein release to just 15% that of WT M. A concomitant loss of binding to Nedd4 ubiquitin ligase was also observed in a GST pull-down assay using the $_{24}$AAAA$_{27}$ mutant of the VSV L domain (23, 37). Furthermore, in contrast to WT VSV M VLPs, Nedd4 was not incorporated into VLPs containing the $_{24}$AAAA$_{27}$ mutation and the mutant M was not ubiquitinated in an *in vitro* ubiquitination assay (23, 25).

Budding efficiency of RV M protein is even more drastically affected by L domain alterations: a recombinant RV expressing a mutation in the $_{35}$PPEY$_{38}$ L domain to $_{35}$SAEA$_{38}$ resulted in the budding efficiency of virions dropping to just 10% of WT RV (33, 81). Electron micrographs showed that the recombinant L domain mutant RV remained cell-associated, indicating the importance of $_{35}$PPEY$_{38}$ in budding.

Paramyxoviruses. Just as the PPxY motif seems to dominate the body of known L domains in filoviruses and rhabdoviruses, the YxxL motif is seemingly more prevalent in the paramyxoviruses. The YxxL motif is sometimes also referred to as the YPxL, Yxxφ

(where φ is any bulky hydrophobic residue), or ØPxV (where Ø is any hydrophobic, aromatic residue) motif (5, 6, 8).

The cellular binding partner for YxxL-containing M proteins, called Alix/AIP1, was first identified with the retrovirus equine infectious anemia virus (EIAV) by a yeast two-hybrid system (7). The use of RNA interference (RNAi) to deplete cellular levels of Alix/AIP1 caused a 60% reduction in EIAV particle release, demonstrating a role for this cellular protein in efficient release of EIAV-infected cells (58).

In 2004, Schmitt et al. identified a new paramyxoviral L domain, $_{20}$FPIV$_{23}$, in the M protein of PIV5 (64). Then, in 2009, Schmitt identified a similar sequence, $_{24}$FPVI$_{27}$, in Mumps virus (MuV), which, like PIV5, belongs to the genus *Rubulavirus* (42). The FPIV-like L domain may be a unique L domain motif or merely an adapted form of the YPxL motif. The phenylalanine instead of tyrosine at the first position is a conservative change (as both amino acids are aromatic and nonpolar) and the presence of a proline at the second position is common in the other L domain motifs (PPxY and YPxL). Similarly, the difference of a valine instead of a leucine at the fourth position represents only a moderate change between these two small, aliphatic amino acids (64). An FPIV-like sequence is not found in all paramyxovirus M proteins, however. In fact, Newcastle Disease virus is the only other paramyxovirus with such a sequence near the amino-terminus of its M protein (42).

Evidence of the L domain function of PIV5's $_{20}$FPIV$_{23}$ sequence is compelling. It is able to restore budding efficiency in L domain-deficient EbV VP40 and HIV Gag and retains functionality when shifted to different sites within PIV5 M protein, an important feature of L domains (64). FPIV-deficient PIV5 viruses lacking either phenylalanine

(F20) or proline (P21) also experience a 20-fold reduction in budding efficiency. However, these mutants quickly compensate for the release deficiency by acquiring second-site reversions to proline that restore L domain activity. Two separate revertants, S369P and L336P, were detected by sequence analysis after recovering viruses that underwent just a single passage in LLC-MK2 cells. Replication was greatly improved for adapted viruses compared with the original mutant virus but was not equivalent to wild-type levels (64). Schmitt et al. speculated that the adaptations, which occurred near the carboxy terminus of PIV5 M protein, might have been the result of the restoration of a proline-based L domain motif, although the context of the flanking amino acids at these two positions does not otherwise bear similarity to any known L domain motifs. The carboxy terminus of matrix proteins from EIAV, HIV-1, HPIV1, HPIV3, and Sendai viruses all also have proline-containing motifs and, in the two retroviruses, these motifs are known L domains.

Results demonstrating L domain activity in MuV $_{24}$FPVI$_{27}$ is still in its early stages, but data suggests that the first three amino acids of $_{24}$FPVI$_{27}$ are critical for M release (42). Alanine substitutions show a decrease in particle release to less than 10% of WT release. However, these findings require further investigation to show that $_{24}$FPVI$_{27}$ has L domain activity, particularly in demonstrating that the sequence can restore budding to an L domain-deficient mutant from another virus.

Ongoing efforts to identify cellular binding proteins for PIV5 M or MuV have identified several unexpected cellular binding partners, but none appear to bind M protein in a FPIV-dependent manner (42). Fluorescence microscopy has shown that MuV M protein does not appear to interact with Alix (42, 64). This lack of interaction with Alix

supports the claim that FPIV is a unique L domain and not a variation of the YxxL motif.

A third paramyxovirus with an identified L domain is Nipah virus (NiV). The $_{62}$YMYL$_{65}$ sequence was first identified by scanning the amino acid sequence of the M protein and locating a pattern similar to EIAV's $_{23}$YPDL$_{26}$ L domain. In-site alanine substitutions of $_{62}$YMYL$_{65}$ to 62-AMYA caused a nearly complete loss of M protein VLP release (8). By appending the YMYL sequence to the carboxy terminus of L domain-deficient EbV VP40, budding efficiency was restored. Appending the AMYA sequence to the budding deficient VP40 did not correct the defect. Another sequence in NiV, $_{92}$YPLGVG$_{97}$ also appears to restore release to budding-deficient EbV VP40, but in an ESCRT-independent manner (57). The authors, Patch et al., speculated that perhaps this peptide uses an alternative mechanism to assist in release and is therefore not a classic L domain.

Sendai Virus Controversy

The budding requirements for the paramyxovirus, SeV, are somewhat controversial due to the publication of two seemingly contradictory reports on the subject. Since SeV and HPIV3 are closely related paramyxoviruses in the same genus, discrepancies concerning SeV particle release bear particular importance to my investigation of HPIV3 budding and thus deserve a more in depth review.

Like the discovery of the YMYL L domain of NiV M protein, the $_{49}$YLDL$_{52}$ L domain of SeV was first identified by scanning the amino acid sequence of SeV M protein to identify close matches to L domain motifs (35). The promising candidate L domain sequence was identified and mutated to 49-AAAA. This mutant demonstrated a 200-fold reduction in VLP release compared to WT SeV M protein.

The authors then attempted to show that the L domain they identified in SeV M protein interacted with Alix/AIP1, consistent with other viral L domains with the YxxL motif. Co-immunoprecipitaton experiments with Alix/AIP1 and SeV M and the appropriate α-SeV M or α-Alix antibodies showed an Alix interaction with M-WT, but not with the 49-AAAA SeV M mutant. A yeast two-hybrid system was also used to successfully demonstrate a direct interaction between WT SeV M protein and Alix/AIP1 (35).

Once the SeV M:Alix/AIP1 interaction had been demonstrated, Irie et al. co-transfected cells with SeV M protein and a DN form of Alix/AIP1 to confirm that functional Alix/AIP1 was critical for efficient M protein VLP release. The DN form of Alix/AIP1 caused a decrease in VLP production to 20% - 40% that of cells expressing functional Alix/AIP1. Using a complementary approach, they then used small interfering RNAs (siRNAs) to deplete Alix/AIP1 from the cells before transfecting them with SeV M. Exhausting Alix/AIP1 by mRNA silencing elicited more than a 10-fold reduction in SeV M protein release (35).

Within months of the Irie et al. paper, Gosselin-Grenet et al. (20) published data that challenged the role of Alix/AIP1 in the release of SeV by using live virus to infect 293T cells rather than expressing SeV M protein alone in 293T cells. In contrast to the findings of Irie et al., the Gosselin-Grenet et al. paper concluded that Alix suppression via siRNA had no effect on the efficient release of SeV particles from infected cells. A key difference between their use of RNAi to suppress Alix and the approach taken by Irie, et al., was that Gosselin-Grenet et al. used a live virus instead of M-WT protein (52).

In addition to investigating the role of Alix in SeV release, Gosselin-Grenet et al. found the expression of a DN form of VPS4 to have no effect on the efficient release of SeV particles. Furthermore, they found no effect on particle release when they expressed DN VPS4 along with anti-Alix siRNAs, which provided strong evidence that SeV does not rely on the same ESCRT proteins for release as other viruses (20). Irie et al. also investigated the role of VPS4 by transfecting cells with a DN form of VPS4, but, instead of infecting with live SeV, the cells were transfected with purified infectious nucleocapsid (34). Consistent with their other experiments, the resulting infectivity of cells expressing DN VPS4 resulted in a significantly lower titer of infectious virus.

One potential reason for the conflicting data may have arisen from different estimations of both transfection and siRNA knockdown efficiency. Anticipating disparities that might arise from variations in transfection efficiency, Gosselin-Grenet et al. used a lentivirus-infected cell line that constitutively expressed GFP-fused anti-Alix siRNAs and GFP-VPS4 fusion proteins to accurately estimate and standardize the levels of protein expression, a measure that Irie et al. did not take. Although the VLP budding assays performed by Irie et al. are standard techniques which have been used by other investigators to publish data on virus release for years, not being able to control and normalize expression of plasmid-encoded M and DN VPS4 in cells – especially co-transfected cells – may have caused the release efficiency estimated from their budding assays to be artificially high.

Another possible explanation for the contradictory results obtained from these two groups was the use of simple transfections to produce M protein-containing VLPs versus live-virus infections that involved a more complex interplay between viral proteins and

the host cell response to infection. The possibility that live SeV exploits a completely separate path in its egress from the host cell from the one taken by lone SeV M protein was offered by Gosselin-Grenet et al. in explanation (20). However this explanation does not address why SeV M would possess a specific mechanism for exiting cells but not use that mechanism in the context of a natural infection. It would not be surprising if the discovery of additional L domains in NiV and SeV, which may provide access to alternate pathways of egress, were made in the near future.

To address this experimental incongruity, in 2010 Irie et al. re-examined the significance of Alix and emphasized the importance of the $_{49}$YLDL$_{52}$ L domain in the context of a live SeV infection (31). By mutating $_{49}$YLDL$_{52}$ to 49-ALDA and 49-AAAA, they observed a 1000-fold decrease in virus titer in both mutants, which was mirrored in previous M protein VLP assays. When propagated in embryonated chicken eggs, a budding-efficient revertant of the 49-ALDA mutant virus was found that had a valine substitution at amino acid 52. This 49-ALDV reversion was put into M protein and shown to interact with Alix as efficiently as wild-type M protein in a mammalian two-hybrid system. In contrast, neither 49-ALDA nor 49-AAAA interacted with Alix. The evidence that SeV utilizes $_{49}$YLDL$_{52}$ to effectively bud from host cells and that the cellular binding partner, Alix, is critical for SeV release is strongly persuasive that this sequence is a genuine L domain.

Both the Irie et al. and Gosselin-Grenet et al. reports relied upon established approaches and tools commonly employed in this line of research, further underscoring the necessity of interpreting data in the context of the experimental conditions adopted. Although we do not yet have a firm explanation for the different results obtained by these

two groups, clearly investigators must be mindful that VLP budding assays, while invaluable, may not reproduce the data yielded from live virus infections.

Summary of Late Domain Identification

To summarize the process of how investigators have typically identified possible L domains and confirmed their functionality, the M protein sequence of a virus is first analyzed to identify sequences that closely resemble known L domain motifs. To test these sequences for L domain activity, alanine-substitution mutants of the candidate L domain and gain-of-function approaches where the candidate L domain is inserted into a matrix protein lacking its own L domain have been used. Further evidence for L domain function can come from using recombinant viruses with alanine substitutions.

Once a functional L domain has been identified, its dependence on a particular cellular factor may be demonstrated by using RNA interference (RNAi) and/or expression of a DN form of the cellular protein target. Yeast two-hybrid systems and co-immunoprecipitation assays are often used to demonstrate a direct interaction between the viral matrix protein and the cellular protein target.

HPIV3 M Protein Release

Much of the material discussed thus far has served to provide pertinent background information about the budding characteristics of viruses related to HPIV3. This section will address what our preliminary data has revealed about the specific budding requirements of HPIV3.

It was important to show that HPIV3 M VLPs were released efficiently from transfected cells, as the establishment of an effective transfection-based HPIV3 M protein budding assay served as the foundation for my research objectives. Preliminary data

confirmed that HPIV3 M protein was released from M plasmid-transfected cells and verified that no other viral proteins were needed for efficient M protein VLP formation (Fig. 5A). The efficiency of HPIV3 M protein release from transfected 293T cells was assessed by comparison to EbV VP40 release, a model for VLP release. Results from this budding assay indicated that ~15% of HPIV3 M protein was released from the cells, which was equivalent to EbV VP40 VLP production (Fig. 5A).

To show that HPIV3 M protein is released from cells in membrane bound VLPs (and not as free proteins), media from cells expressing M protein was treated enzymatically, with and without the presence of the membrane-solubilizing detergent Triton X-100 and immunoprecipitated with α-HPIV3 M. M protein was digested only when the solubilization of the membrane rendered M protein susceptible to trypsin digestion (Fig. 5B). This showed that M protein was released from the transfected cells as a membrane-enveloped VLP.

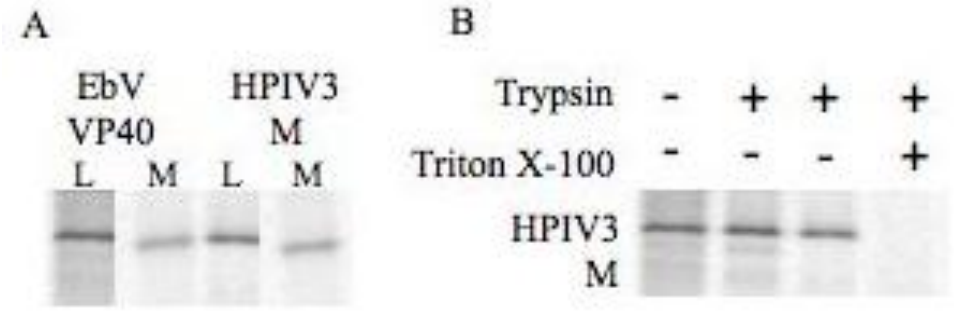

Fig. 5. HPIV3 M protein is able to efficiently release from cells as VLPs. A. Relative levels of EbV VP40 protein and HPIV3 M protein in both the cellular lysate (L) and the media (M). Roughly 15% of HPIV3 M protein is released from the transfected cells. B. HPIV3 M releases as membrane enveloped VLPs. M proteins are not susceptible to trypsin digestion without first having the enveloping lipid membrane of the VLP solubilized by detergent-treatment.

Since we suspected that HPIV3 is a canonical, VPS pathway-utilizing virus, we also wanted to demonstrate that ubiquitin depletion would cause a reduction in budding. Treatment with the ubiquitin-depleting drug, MG132, did not affect synthesis of viral proteins and caused a 5-fold decrease in HPIV-3 virus release (Fig. 6). This 5-fold decrease in budding was also observed when comparing the titers of virus particles released from MG132-treated cells to those released from untreated cells. This suggests that ubiquitination is important for HPIV-3 particle release.

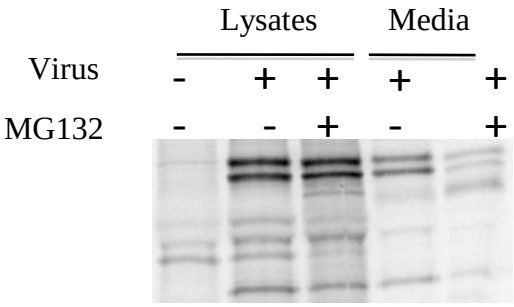

Fig. 6. Treatment with MG132 impedes the releases of HPIV3 particles. Cell were infected with HPIV3 at an MOI of 3 and treated with 20 μM MG132. At 9 hpi, infected cells were radiolabeled and allowed to incubate for an additional 18 h before collecting the media and lysing the cells. The cellular lysates and media were collected and immunoprecipitated with α-HPIV3. Precipitated proteins were separated by SDS-PAGE and analyzed by phosphoimager.

This preliminary evidence indicated that HPIV3 buds from cells in a manner similar to many related viruses, suggestive of the presence of an L domain that enables the M protein to interact with components of the MVB pathway. The fact that many L domains have been identified in close relatives of HPIV3 further justifies the pursuit of identifying an L domain in HPIV3 M protein. This was the overarching objective of my research.

CHAPTER II

RESEARCH OBJECTIVES

Characterizations of viral matrix proteins and their interactions with cellular trafficking proteins have contributed significantly to the fields of cell biology and virology. More importantly, our understanding of viral assembly and release processes also offer us targets for the development of new antiviral drugs.

The L domains of many viruses have been identified. However, none of these known L domains are found in the HPIV3 M protein. Therefore, the focus of my investigation will be to identify the L domain(s) of HPIV3 M protein by assaying four candidate sequences for L domain activity.

Thus, my specific aims are to:

1. Identify, mutate, and characterize the budding efficiency of potential HPIV3 M protein L domains.
2. Confirm L domain activity of candidate sequences by functional restoration assays.

CHAPTER III

MATERIALS AND METHODS

Plasmid Construction

A QuikChange site-directed mutagenesis kit (Stratagene) was used to make alanine-substitution mutations (APKH, ALDV, KPEA, APNI) in a pCAGGS-M-WT plasmid. The pCAGGS plasmid is mammalian, high expression vector.

The pCAGGS-VP40-WT and pCAGGS-VP40-ΔPT/PY plasmids were provided by Dr. Ronald Harty, University of Pennsylvania – Philadelphia (32). A series of pCAGGS-VP40-dPT/PY mutants were made that contained inserts with the three flanking amino acids from each side of HPIV3's candidate L domain sequences cloned directly into the deletion site. Another series of pCAGGS-VP40-ΔPT/PY mutants containing the inserted sequences from HPIV3 M was also cloned into the carboxy terminal end of VP40, just before the stop codon. The amino terminal deletion construct with the first 13 amino acids of VP40 removed (VP40-ΔN13) was generated using PCR directed mutagenesis, and the PCR products were cloned into pCAGGS-VP40. The PTAPPEY and HPIV3 candidate L domains (with the four flanking amino acids from each side of the insert) were appended to the carboxy terminus of VP40-ΔN13 using PCR-based mutagenesis. All mutations were confirmed by sequencing by Eton Biosciences in San Diego, California.

Budding Assay

Budding experiments were done using 293T cells, a highly transfectable human cell line derived from embryonic kidney cells that we used successfully in previous experiments (63). 293T cells in standard 6-well plates were grown to 70%-80% confluency in Dulbecco's modified Eagle medium (DMEM) containing 10% fetal bovine serum (FBS). The cells were transfected using Lipofectamine LTX with Plus reagent (Invitrogen) according to the manufacturer's instructions. For experiments with pCAGGS-M, the following amounts of pCAGGS plasmids were used: 0.9 μg M-WT, 0.75 μg M-APKH, 1.0 μg M-ALDV, 2.0 μg M-KPEA, and 2.0 μg M-APNI. The plasmid amounts varied to compensate for varying levels of protein expression from the plasmids. At 24 hours post-transfection, the 10% FBS DMEM was removed and replaced with a methionine-free media to exhaust the methionine available to the cells for protein synthesis. After 30 minutes, the cells were radiolabeled with 40 μCi (or 4 μl/well) of [^{35}S] methionine (Pro-mix-[^{35}S] *in vitro* cell labeling mix, Amersham Biosciences) and incubated for an additional 20 hours to ensure time for the incorporation of radiolabeled isotope in protein synthesis and budding M VLPs.

After this incubation period, the media was collected and the cells lysed with 400 μl cell lysis buffer (0.5% NP-40, 20 mM Tris-HCl [pH 7.4], 150 mM NaCl, Promega). Media and cell lysate samples were centrifuged at low speed to separate cellular debris and then the media was treated with 0.5% Triton X-100 to solubilize the membranes of VLPs. Lysate and media samples were incubated for two hours with an antibody against M protein (provided by Dr. Amiya Banerjee, Cleveland Clinic) and 25 μl of protein A agarose resin (Thermo Scientific). (The α-HPIV3 antibody shows specificity for HPIV3

M, N, and HN proteins, but, as only M protein is used in this assay, it is effective for use in this in these experiments).

Following incubation, complexes of protein A beads-antibody-M protein were pelleted and washed four times with radioimmunoprecipitation assay buffer (25 mM Tris-HCl [pH 7.6], 150 mM NaCl, 1% NP-40, 1% sodium deoxycholate, 0.1% SDS; Thermo Scientific) then resuspended in 25 μl of 2X SDS buffer. Radiolabeled proteins were then separated by SDS-PAGE. The gels were dried and later visualized by phosphorimager analysis on a Storm 860 Molecular Imager. ImageQuant software provided the means of quantifying protein levels detected in the media and in the lysate fractions.

For the VP40 experiments, cells were transfected with 1.2 μg of plasmid for all constructs of pCAGGS-VP40. After radiolabeling as described above, cells were lysed and the lysates were immunoprecipitated with a monoclonal α-VP40 antibody provided by Dr. Yoshihiro Kawaoka at the University of Wisconsin – Madison (53, 55). Instead of immunoprecipitation, the media in the VP40 series of experiments was clarified briefly with a low-speed spin, layered onto a 20% sucrose cushion, and ultracentrifuged at 186,000 x g, 4 °C, for 2 h. Proteins from the lysate and media fractions were visualized as described above.

CHAPTER IV

RESULTS

Aim 1. Identify, Mutate, and Characterize Potential HPIV3 M Protein L Domains

To identify an L domain in the HPIV3 M protein, I scanned the HPIV3 M protein sequence and selected four potential L domain sequences to investigate: $_{47}$PPKH$_{50}$, $_{54}$YLDV$_{57}$, $_{135}$KPEL$_{139}$, and $_{338}$YPNI$_{341}$. These were selected based on their sequence similarity to known L domains (Appendix A). To determine whether any of our four potential L domain candidates were functional, alanine substitutions were created at each site in a pCAGGS plasmid encoding the HPIV3 M gene (Fig. 7). The mutations created were previously shown to significantly disrupt L domain function in other M proteins.

Potential HPIV3 L domain:	$_{47}$PPKH$_{50}$	$_{54}$YLDV$_{57}$	$_{135}$KPEL$_{138}$	$_{338}$YPNI$_{341}$
L domain motif:	PPxY	YxxL	YxxL	YxxL
Proposed mutations of HPIV3 M:	47-APKH	54-ALDV	135-KPEA	338-APNI

Fig. 7. Potential HPIV3 M protein L domains and corresponding substitution mutants.

Of the potential L domains, disruption of $_{47}$PPKH$_{50}$ and $_{338}$YPNI $_{341}$ appeared to have the least effect on M VLP release. The 47-APKH and 338-APNI mutants released at 100% and 75% the efficiency of M-WT, respectively. Mutations in the $_{54}$YLDV$_{57}$ and $_{135}$KPEL$_{138}$ sequences had a more drastic effect on M VLP release: the 54-ALDV and 135-KPEA mutants were released into the media at only 30 - 40% and less than 20% the efficiency of M-WT, respectively (Fig. 8A).

Although the 135-KPEA mutant was released at lower levels than any of the other constructs in the series, it was also expressed at lower levels in cells. In fact, even when cells were transfected with plasmid volumes 2 to 3-fold higher than the other constructs, 135-KPEA was not detected at equivalent levels in the lysates. This may have been due to a destabilizing effect of the mutation on the protein's overall stability. Regardless, the lower expression undermines any significance of the low release of the 135-KPEA mutant.

The possibility that HPIV3 M protein has two L domains must also be considered. For example, if $_{54}$YLDV$_{57}$ and $_{338}$YPNI$_{341}$ both function as L domains, release of the 338-APNI mutant may have remained efficient due to the second redundant L domain ($_{54}$YLDV$_{57}$) that retained budding activity. My second aim, described in the following section, was devised in part to circumvent the experimental limitations of these alanine-substituted mutants and confirm positive results.

A

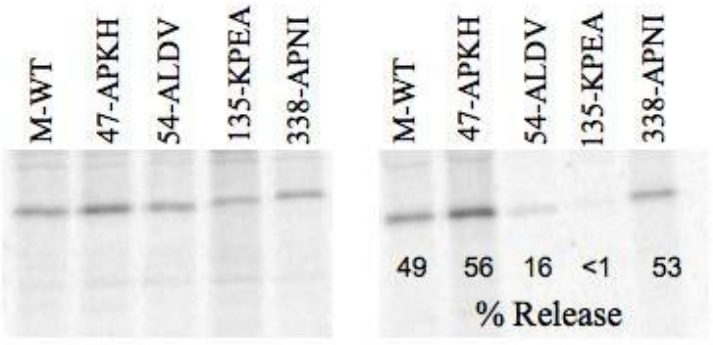

Lysates Media

B

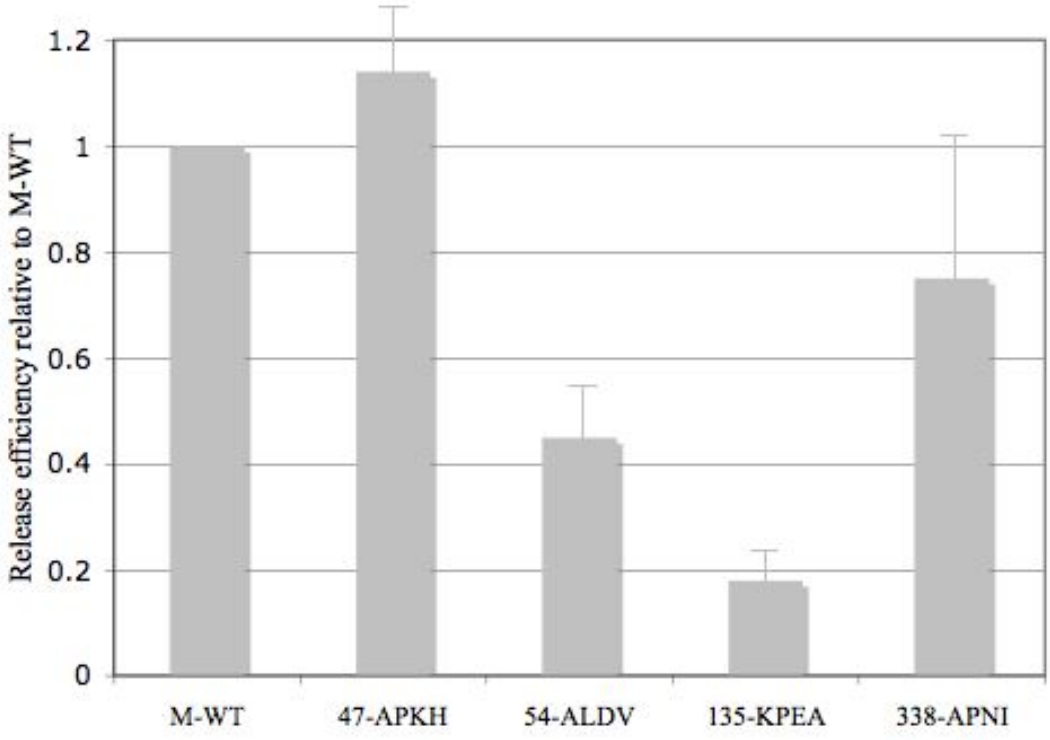

Fig. 8. Budding of HPIV3 M proteins containing mutations in potential L domains. A. Sample experiment of the alanine substitution mutants compared to M-WT. Cells expressing pCAGGS M and mutants were lysed and media collected 48 hpt. Both lysates and media were immunoprecipitated with α-HPIV3. Band intensities reflecting relative M protein quantities were calculated using Storm Imager analysis. The percent release reflects the data from this single experiment and was calculated by dividing the amount of M detected in the media by the total amount of M protein (detected in both the media and the lysate fraction). B. Release efficiency of each mutant was normalized to M-WT. Quantification of results taken from the average of three experiments with error bars.

Aim 2. Confirm L Domain Activity of Candidate Sequences by Functional Restoration Assays

To confirm the results of the first objective and clarify ambiguous results, a complementary gain-of-function approach was also employed. Since functional L domains are able to restore budding to L domain-deficient matrix proteins of other viruses, we designed an experiment to investigate whether any of our four candidate sequences could restore budding when inserted into EbV VP40 lacking its $_{7}$PTAPPEY$_{13}$ L domain (VP40-ΔPT/PY) (Fig. 9A).

For this series of experiments, EbV VP40 was selected as a model matrix protein because several other researchers had used the poorly budding VP40-ΔPT/PY mutant to show that the insertion of L domains from different viruses can restore budding efficiency (8, 64). VP40 VLP release is also well characterized, having been verified by flotation analysis, trypsin-resistance assays, and electron microscopy (55, 71).

Using the VP40-ΔPT/PY plasmid to vector the HPIV3 sequences, we designed two sets of VP40 mutants: in the internal insertion series, the four potential L domain sequences and three flanking residues were inserted directly into the L domain deletion site. In the second, C-terminal insertion series, the same HPIV3 sequences were cloned into carboxy terminus, just upstream of the VP40 stop codon.

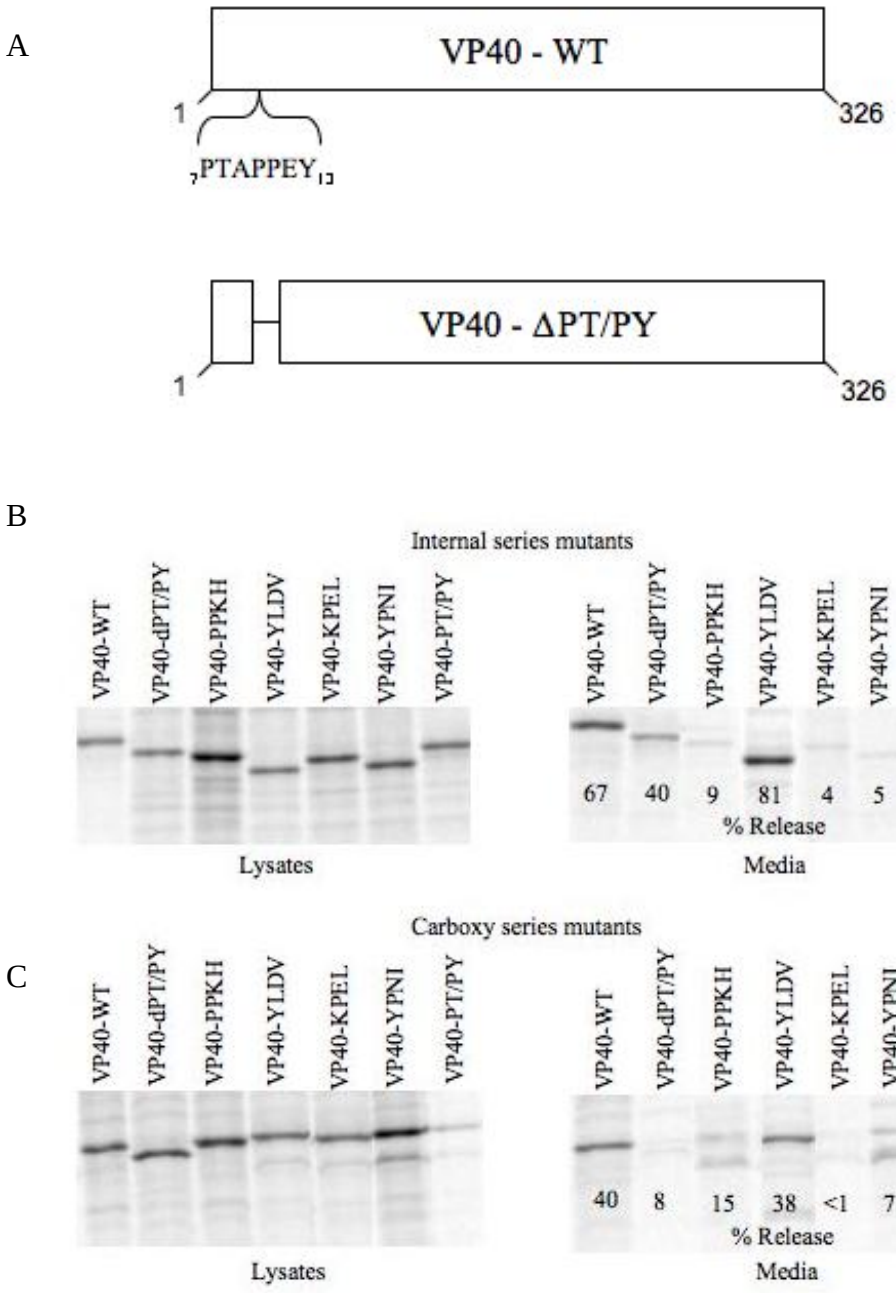

Fig. 9. The HPIV3 sequence YLDV is able to enhance release of VP40-ΔPT/PY. A. HPIV3 candidate sequences were inserted onto the carboxy terminus of a parental VP40 mutant lacking its PTAPPEY L domain. Internal (B) and carboxy terminal (C) series VP40 experiments where cells were transfected with 1.2 μg of each pCAGGS-VP40 construct, radiolabeled at 24 hpt, and lysed at 48 hpt. Media was clarified briefly and the supernatant ultracentrifuged at 4°C, 186,000 x g for 2h. Lysates were immunoprecipitated with α-VP40. Proteins were separated by SDS-PAGE and visualized by phosphoimager analysis.

The $_{54}$YLDV$_{57}$ sequence was able to improve budding efficiency of VP40-ΔPT/PY when inserted into the internal site (9B) and appended to the carboxy terminus (9C), while the $_{47}$PPKH$_{50}$, $_{135}$KPEL$_{138}$, and $_{338}$YPNI$_{341}$ sequences did not restore budding in either context. While these trends were observed throughout several repeat experiments, there were several major issues with the experiment.

One issue was that the results for both the internal and carboxy terminal series were surprisingly variable, which produced unacceptably high standard deviations (Fig. 10). Second, the carboxy terminal addition of PT/PY did not produce the expected restoration of VP40 budding (others have reported a 4 to 5-fold increase in release relative to VP40-WT with the same construct) (44). Finally, and most importantly, the parental construct for this experiment, VP40-ΔPT/PY, budded much more efficiently than expected. This was especially problematic because it made the restoration ability of each candidate L domain more difficult to assess.

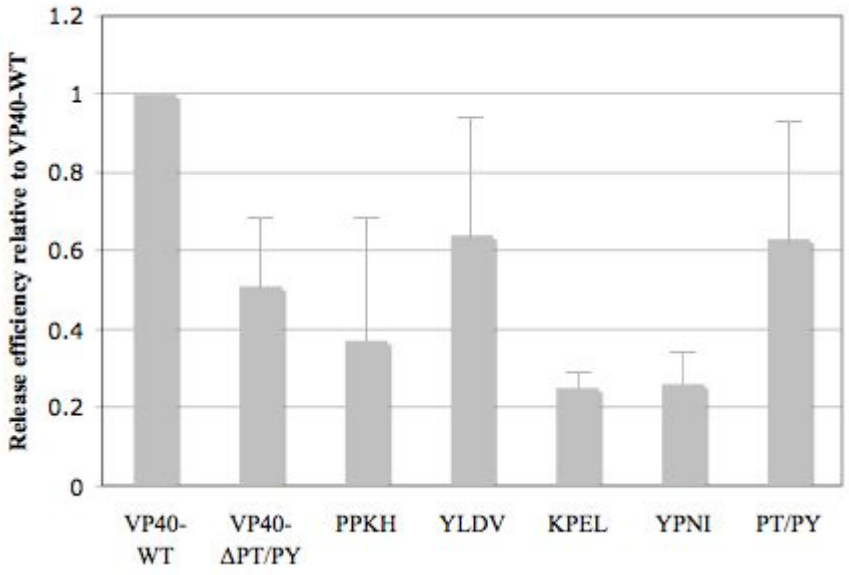

Fig. 10. Budding restoration assays with C-terminal addition of potential L domains to VP40-ΔPT/PY. The data reflects the average release efficiency of each carboxy terminal VP40 mutant relative to VP40-WT for three experiments.

Due to this unexpectedly high level of VP40-ΔPT/PY VLP release in these preliminary experiments, we created a new parental VP40 construct in which the first 13 residues of the amino terminus were deleted (VP40-ΔN13) (Fig. 11A). The release of the VP40-ΔN13 mutant was less efficient than the release of VP40-ΔPT/PY, especially at lower plasmid concentrations (Fig. 11B). Based on the more severe defect caused by this deletion, VP40-ΔN13 appeared to be a more suitable vector for the restoration experiments.

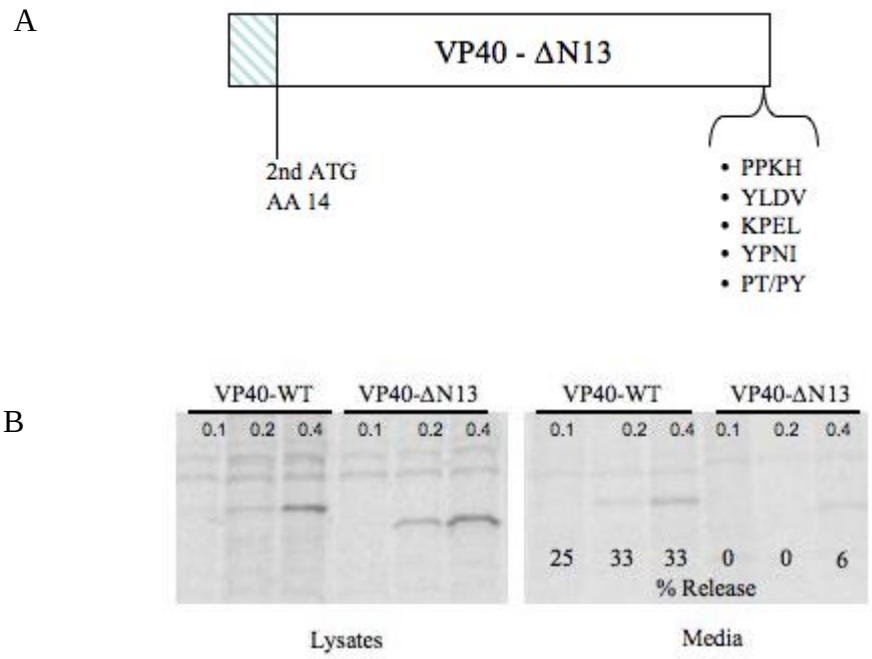

Fig. 11. VP40-ΔN13 has reduced budding relative to VP40-WT. A. The first 13 residues from the amino terminus were removed to create another budding deficient form of VP40 (VP40-ΔN13). B. Budding curve of VP40-WT and VP40-ΔN13. Constructs were expressed in cells at 0.1 μg, 0.2 μg, and 0.4 μg. Cells were radiolabeled at 24 hpt and lysed at 48 hpt. Media was clarified briefly and the supernatant ultracentrifuged at 4°C, 186,000 x g for 2 h. Lysates were immunoprecipitated with α-VP40. Proteins were separated by SDS-PAGE and visualized by phosphoimager analysis.

When the HPIV3 L domain candidate sequences were appended to the carboxy terminus of VP40-ΔN13 and expressed at equivalent levels, the $_{54}$YLDV$_{57}$ sequence demonstrated L domain activity by restoring release efficiency to VP40-WT levels (Fig. 12). The $_{47}$PPKH$_{50}$ and $_{338}$YPNI$_{341}$ sequences showed slight, but not significant, increases in release efficiency, while the $_{135}$KPEL$_{138}$ sequence had a negative effect on release. As observed with the VP40-ΔPT/PY vector, appending the natural $_{7}$PTAPPEY$_{13}$ sequence of EbV VP40 to the carboxy terminus did not restore release to WT levels.

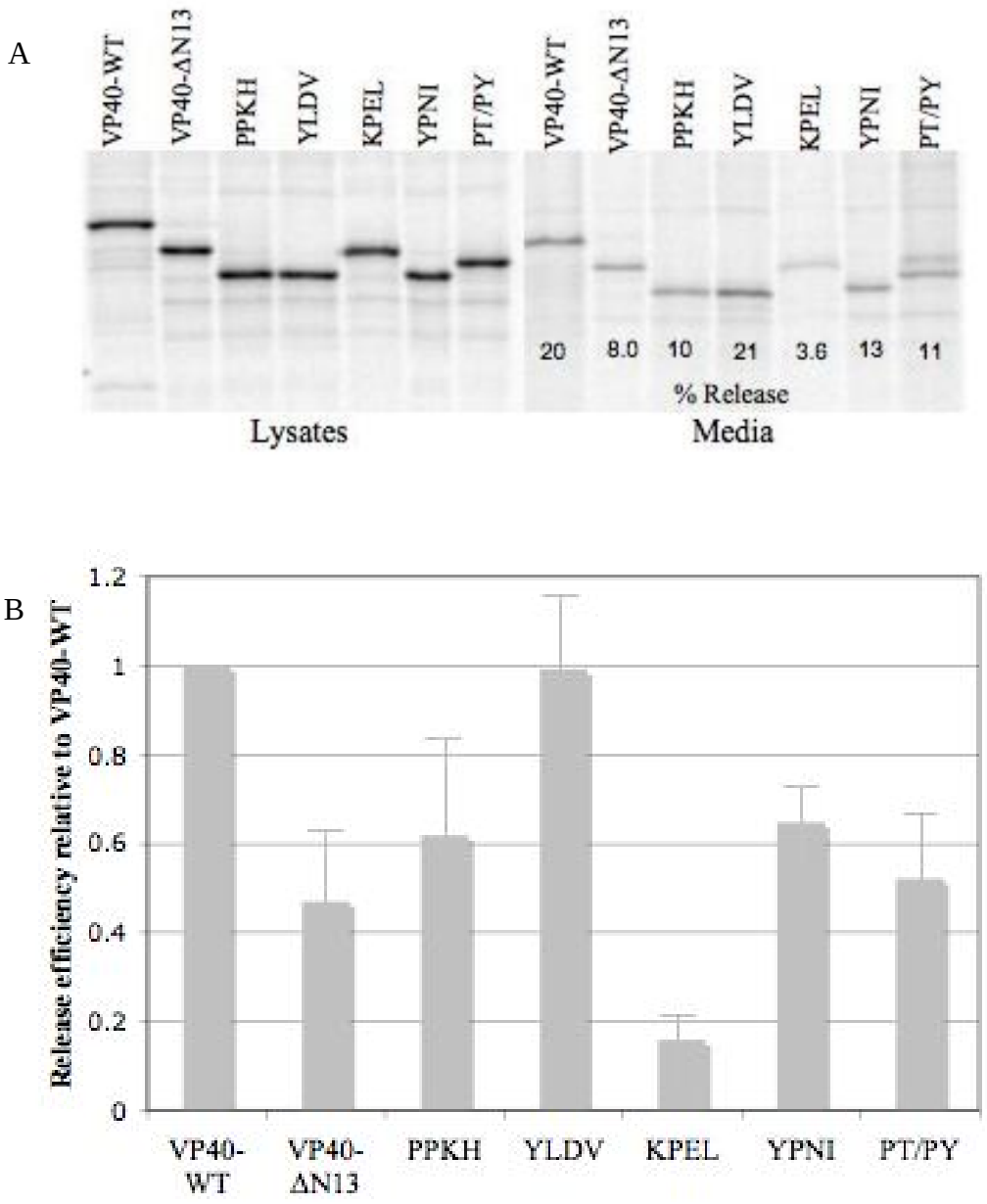

Fig. 12. Appending YLDV to the carboxy terminus of VP40-ΔN13 restored budding to near wild-type levels. A. 293T cells were transfected with VP40, radiolabeled at 24 hpt, and lysed at 48 hpt. The media was briefly clarified and the supernatant was layered onto 20% sucrose before being ultracentrifuged at 4°C, 186,000 x g, for 2 h. The lysates were immunoprecipitated with α-VP40. Proteins were separated by SDS-PAGE and visualized by phosphoimager analysis. B. Release efficiency of each mutant was normalized to VP40-WT. Quantification of results was calculated from the average of three experiments with release efficiencies normalized to VP40-WT.

CHAPTER V

DISCUSSION

Through our combined approaches designed to identify an HPIV3 L domain, four candidate sequences were subjected to a rigorous evaluation of L domain activity. This study provides strong evidence that $_{54}$YLDV$_{57}$ functions as an L domain in the HPIV3 M protein. This is due to its (i) position and sequence similarity to the $_{49}$YLDL$_{53}$ L domain of SeV, (ii) twofold decrease in budding efficiency when mutagenized to ALDV, and (iii) ability to restore budding to wild-type levels in a budding deficient VP40.

To further analyze the $_{49}$YLDL$_{53}$, M protein sequences from the *Respirovirus*, *Morbillivirus* and *Henipavirus* genera of *Paramyxoviridae* were aligned (Appendix A). While these three genera are not particularly closely related within the *Paramyxoviridae*, their M proteins align fairly well. Furthermore, SeV and NiV are the only viruses within the family besides PIV5 (whose M protein aligns very poorly with HPIV3 M) with known L domains. A Yxxφ pattern is consistently present in the alignments near the amino terminus. Although the amino terminal Yxxφ sequences of these viruses do not share a perfect consensus, the $_{54}$YLDV$_{57}$ sequence of HPIV3 and the $_{49}$YLDL$_{53}$ and $_{62}$YMYL$_{65}$ L domains of SeV and NiV, respectively, are positionally similar and possess the YxxL motif (with the conservative amino acid difference of a valine instead of a leucine).

In contrast to $_{54}$YLDV$_{57}$, we found no evidence of L domain activity in $_{47}$PPKH$_{51}$. The 47-APKH M mutant had release efficiency on par with, or even better than, M-WT, and PPKH had a negligible effect on enhancing the budding efficiency of VP40-ΔN13. Furthermore, the fourth position difference between the histidine of $_{47}$PPKH$_{51}$ and the tyrosine in the PPxY motif is ranked as fairly dissimilar residues in substitution matrices.

We also found the $_{135}$KPEL$_{138}$ sequence to be devoid of L domain activity. While the release of the 135-KPEA M mutant appeared low in Fig. 8 and other experiments, we had trouble expressing it at equivalent levels, possibly due to protein misfolding/instability caused by the alanine-substitution. Still, KPEL had no budding restorative effects when inserted into budding-deficient VP40.

The possibility that this $_{135}$KPEL$_{138}$ sequence possessed L domain activity was supported by its second position proline. Prolines are common residues in viral L domains (e.g. YPDL, PTAPPEY, PPPY, FPIV/FPVI) and, in PIV5, were shown to enhance the release of virions when supplemental proline residues were cloned into the M protein (64). However, unlike $_{47}$PPKH$_{51}$, the alignment of $_{135}$KPEL$_{138}$ with even closely related viruses is poor (Appendix A) and its initial selection as a candidate L domain for study was based on the admittedly loose sequence association with the $_{484}$YPDL$_{487}$ L domain of EIAV.

Evidence supporting L domain activity in $_{338}$YPNI$_{341}$ was more equivocal because we could not rule out the possibility that it might act as a secondary L domain in HPIV3. Its position in the carboxy terminus of M protein aligns well with the nine other paramyxoviruses in Fig. 13, which, with the exception of BPIV3's identical $_{338}$YPNI$_{341}$ tetrapeptide, all maintain a YxxV pattern in this position. Although its ability to

enhance release of VP40-ΔN13 was significant, albeit slight, the negative effect of 338-APNI on M release was marginal and highly variable. Overall, evidence leans against $_{338}$YPNI$_{341}$ being an L domain, but further investigation is warranted.

There are several ways we could further analyze these sequences for L domain activity. First, we could create and analyze recombinant viruses having mutations in $_{54}$YLDV$_{57}$ and/or $_{338}$YPNI$_{341}$. If either or both of these sequences serve as L domains, it should result in slower replicating viruses with impaired release. Furthermore, if slow growing viruses are observed, it may be possible to isolate large plaque revertants from them. Sequence analysis of such adapted viruses may reveal changes that restore L domain and budding efficiency.

Second, we could insert the potential L domains into another budding deficient protein to confirm the VP40 restoration experiments. The HIV-1 Gag protein would be an excellent M model to adapt for our purposes because much of what is known about the budding of enveloped viruses was pioneered using Gag. Gag might also be a better system because it could help to circumvent the some of the drawbacks we encountered using EbV VP40. Finally, it would be ideal to reproduce our VP40 results to simply reinforce their validity, just as Schmitt et al. did when they used L domain-deficient forms of Gag and VP40 for inserting PIV5 L domain candidates (64).

Third, further mutagenesis analysis of $_{54}$YLDV$_{57}$ will help to solidify its identity as a Yxxφ-type L domain. If it is indeed an L domain, analyzing alanine substitution mutations that scan the tetrapeptide should show that the conserved first position tyrosine is especially sensitive to substitution. We will also characterize the residues in $_{338}$YPNI$_{341}$ by mutagenesis in an M protein background in which $_{54}$YLDV$_{57}$ is mutated.

A fourth way to confirm L domain activity and investigate the mechanism of budding would be to demonstrate the functional and physical interaction between HPIV3 M and Alix. Since both the $_{54}$YLDV$_{57}$ and $_{338}$YPNI$_{341}$ sequences have the Yxxφ-type motif, demonstrating an L domain-dependent interaction would also confirm L domain function. The physical interaction could be confirmed using mammalian two-hybrid systems, GST pull-downs, or co-immunoprecipitation assays. Additionally, to assess the importance of Alix in HPIV3 release, we could knockdown cellular levels of Alix by using either siRNA or DN Alix. Recalling the difficulties experienced by the SeV researchers in assessing the role of Alix in release, the effect of Alix depletion should be analyzed in both M budding assays and live virus infections. This would also be relevant in reconciling the controversial requirement of Alix for SeV budding.

These future experiments will be especially important in confirming the L domain activity of $_{54}$YLDV$_{57}$ given the unexpected difficulties we experienced with the VP40-based restoration experiments. We were surprised at the high level of VP40-ΔPT/PY release and initially questioned the validity of our results. However, after confirming that our mutant VP40 had the correct amino terminal deletion of $_{7}$PTAPPEY$_{13}$, we reviewed the literature on EbV budding and found more variability in the budding efficiency of L domain-deficient VP40 than we were previously aware of.

The following discussion illustrates some of the discrepant results that make the importance of $_{7}$PTAPPEY$_{13}$ in VP40 release unclear. Licata et al. found that deleting the entire $_{7}$PTAPPEY$_{13}$ L domain, just as we did, resulted in a reduction in VP40 VLP release to just 1% of WT (44). Likewise, another group found that a mutated version of $_{7}$PTAPPEY$_{13}$ (7-PTAAAEY) caused a reduction in VP40 release to 6% of WT (64).

However, Licata et al., the same group to report a near complete loss of budding in their VP40-ΔPT/PY mutant, found that deleting the Tsg101-binding L domain, $_{7}$PTA$_{9}$, actually enhanced VP40 release to 135% of WT. Furthermore, substituting an alanine for proline at the first proline (7-ATAPPEY) improved release to 123% of WT (44).

Other groups have also found deletions or mutations of $_{7}$PTAPPEY$_{13}$ to have less pronounced effects on VP40 release. One report found that VP40 with a 10-AAEY mutation released at approximately 30% the efficiency of VP40-WT (85). Two additional reports underscored the variability of VP40 release efficiency: one reported that a VP40-Δ30 mutant budded at 20% the efficiency of WT (71) while another found that a VP40-Δ50 mutant still released into the media at roughly 25% - 30% the levels of VP40-WT (84). Our own VP40-Δ13 mutant released at roughly 25% the efficiency of VP-WT. Consistent with these findings, a recombinant EbV containing mutations in both L domains is still viable, though it replicates at a decreased rate (53).

There are a number of experimental variables may influence release efficiencies of budding-deficient VP40 mutants. Particulars such as whether the flanking sequences of inserts were transferred into the budding-deficient VP40 vector, which molecular tags were appended to the VP40 constructs, incubation times, and which transfection reagents, cell lines and plasmid concentrations were used for transfections, varied from one group to another. Since VP40-based restoration systems have been used to characterize the L domains in several viruses, it is surprising that these varying results in the literature haven't been more thoroughly scrutinized and that more of an effort to standardize an experimental design hasn't been made (8, 64). Despite these variables, our experimental design still produced strong evidence of an L domain in a VP40-based restoration system

that was consistent with data from our mutagenesis experiments. Still, the lack of sensitivity and responsiveness in the budding-deficient vector further confirms the need to repeat restoration experiments with a retroviral Gag system.

While we began this research with the widely accepted assumption that understanding the L domain-mediated interaction with an ESCRT protein was the key to understanding the broader mechanism of budding, since the onset of this project there has been an ever greater recognition that the budding of enveloped viruses is more varied and than previously thought.

One complicating factor is the presence of multiple viral L domains. Viruses with multiple L domains, such as HIV-1, MARV and EbV, and Lassa virus, are able to bind to different ESCRT proteins and have been shown to retain budding ability when one L domain is compromised through the compensatory actions of a second L domain (18, 44, 45, 70, 72, 73). Another consideration is recent evidence that at least one viral matrix protein, the M2 protein of influenza, is able to provide its own driving force for budding and thus bypass the need for ESCRT proteins altogether (19, 60). Viruses whose release appears to be unaffected by the depletion of VPS4/expression of DN VPS4, including VSV, possibly SeV, respiratory syncytial virus, and influenza, support the notion that budding may occur via an alternate, ESCRT-independent mechanism (7, 20, 60, 75). Finally, many of the viral M proteins discussed in this thesis, such as SeV, EbV, and PIV5, depend on the co-expression of accessory proteins for efficient budding (61, 64, 72). In the case of MARV, even though the virus has a "traditional" $_{16}$PPPY$_{19}$ L domain in VP40, a bonafide Tsg101-interacting PSAP L domain has also been identified on the NP protein (11).

We are just beginning to characterize interactions that occur during live virus infections that may supplant or augment the interactions of a single M protein. In the larger picture of virus release, defects in any number of important M protein functional domains (including L domains, membrane targeting motifs, oligomerization sites, etc.) may also affect the efficient release of VLPs or virions. Due to the presence of redundant and compensatory mechanisms, however, these defects rarely destroy release altogether, and the ability of L domain-deficient M proteins to escape from the host cell, even at greatly reduced efficiency, would be very difficult to explain without considering the possibility that virus's have evolved multiple strategies to ensure the success of this final important step in their life cycle.

CHAPTER VI

CONCLUSION

In summary, $_{54}$YLDV$_{57}$ demonstrated L domain activity in mutagenesis and restoration experiments, while the $_{47}$PPKH$_{50}$ and $_{135}$KPEL$_{138}$ sequences did not exhibit any L domain activity. Since the presence of multiple L domains is well characterized in many distantly related viruses, we are especially intrigued by the moderate L domain activity demonstrated by $_{338}$YPNI$_{341}$. We intend to investigate this possible L domain further in expanded mutagenesis and restoration assays.

REFERENCES

1. **[Anon], and CDC.** 1999. Epidemiology of measles - United States, 1998 (Reprinted from MMWR, vol 48, pg 749-753, 1999). Jama-Journal of the American Medical Association 282:1323-1324.

2. **Ali, A., and D. P. Nayak.** 2000. Assembly of Sendai virus: M protein interacts with F and HN proteins and with the cytoplasmic tail and transmembrane domain of F protein. Virology **276**:289-303.

3. **Babst, M.** 2005. A protein's final ESCRT. Traffic **6**:2-9.

4. **Babst, M.** 2006. A close-up of the ESCRTs. Dev Cell **5**:547-8.

5. **Bieniasz, P. D.** 2006. Late budding domains and host proteins in enveloped virus release. Virology **344**:55-63.

6. **Chen, B. J., and R. A. Lamb.** 2008. Mechanisms for enveloped virus budding: can some viruses do without an ESCRT? Virology **372**:221-32.

7. **Chen, C., O. Vincent, J. Jin, O. A. Weisz, and R. C. Montelaro.** 2005. Functions of early (AP-2) and late (AIP1/ALIX) endocytic proteins in equine infectious anemia virus budding. J Biol Chem **280**:40474-80.

8. **Ciancanelli, M. J., and C. F. Basler.** 2006. Mutation of YMYL in the Nipah virus matrix protein abrogates budding and alters subcellular localization. J Virol **80:**12070-8.

9. **Coronel, E. C., T. Takimoto, K. G. Murti, N. Varich, and A. Portner.** 2001. Nucleocapsid incorporation into parainfluenza virus is regulated by specific interaction with matrix protein. J Virol **75:**1117-23.

10. **Craven, R. C., R. N. Harty, J. Paragas, P. Palese, and J. W. Wills.** 1999. Late domain function identified in the vesicular stomatitis virus M protein by use of rhabdovirus-retrovirus chimeras. J Virol **73**:3359-65.

11. **Dolnik, O., L. Kolesnikova, L. Stevermann, and S. Becker.** 2010. Tsg101 is recruited by a late domain of the nucleocapsid protein to support budding of Marburg virus-like particles. J Virol **84**:7847-56.

12. **Durbin, A. P., and R. A. Karron.** 2003. Progress in the development of respiratory syncytial virus and parainfluenza virus vaccines. Clin Infect Dis **37**:1668-77.

13. **Ebata, S. N., L. Prevec, F. L. Graham, and K. Dimock**. 1992. Function and immunogenicity of human parainfluenza virus 3 glycoproteins expressed by recombinant adenoviruses. Virus Res **24**:21-33.

14. **Falsey, A. R., and E. E. Walsh.** 2006. Viral pneumonia in older adults. Clin Infect Dis **42**:518-24.

15. **Fouillot-Coriou, N., and L. Roux.** 2000. Structure-function analysis of the Sendai virus F and HN cytoplasmic domain: different role for the two proteins in the production of virus particle. Virology **270**:464-75.

16. **Fry, A. M., A. T. Curns, K. Harbour, L. Hutwagner, R. C. Holman, and L. J. Anderson.** 2006. Seasonal trends of human parainfluenza viral infections: United States, 1990-2004. Clin Infect Dis **43**:1016-22.

17. **Gao, J., B. P. De, and A. K. Banerjee.** 1999. Human parainfluenza virus type 3 up-regulates major histocompatibility complex class I and II expression on respiratory epithelial cells: involvement of a STAT1- and CIITA-independent pathway. J Virol **73**:1411-8.

18. **Garrus, J. E., U. K. von Schwedler, O. W. Pornillos, S. G. Morham, K. H. Zavitz, H. E. Wang, D. A. W**ettstein, K. M. Stray, M. Cote, R. L. Rich, D. G. Myszka, and W. I. Sundquist. 2001. Tsg101 and the vacuolar protein sorting pathway are essential for HIV-1 budding. Cell **107**:55-65.

19. **Gomez-Puertas, P., C. Albo, E. Perez-Pastrana, A. Vivo, and A. Portela.** 2000. Influenza virus matrix protein is the major driving force in virus budding. J Virol **74**:11538-47.

20. **Gosselin-Grenet, A. S., J. B. Marq, L. Abrami, D. Garcin, and L. Roux.** 2007. Sendai virus budding in the course of an infection does not require Alix and VPS4A host factors. Virology **365**:101-12.

21. **Gottlinger, H. G., T. Dorfman, J. G. Sodroski, and W. A. Haseltine.** 1991. Effect of mutations affecting the p6 gag protein on human immunodeficiency virus particle release. Proc Natl Acad Sci U S A **88**:3195-9.

22. **Gubbay, O., J. Curran, and D. Kolakofsky.** 2001. Sendai virus genome synthesis and assembly are coupled: a possible mechanism to promote viral RNA polymerase processivity. J Gen Virol **82**:2895-903.

23. **Harty, R. N., M. E. Brown, J. P. McGettigan, G. Wang, H. R. Jayakar, J. M. Huibregtse, M. A. Whitt, and M. J. Schnell.** 2001. Rhabdoviruses and the cellular ubiquitin-proteasome system: a budding interaction. J Virol **75**:10623-9.

24. **Harty, R. N., M. E. Brown, G. Wang, J. Huibregtse, and F. P. Hayes.** 2000. A PPxY motif within the VP40 protein of Ebola virus interacts physically and functionally with a ubiquitin ligase: implications for filovirus budding. Proc Natl Acad Sci U S A **97**:13871-6.

25. **Harty, R. N., J. Paragas, M. Sudol, and P. Palese.** 1999. A proline-rich motif within the matrix protein of vesicular stomatitis virus and rabies virus interacts with WW domains of cellular proteins: implications for viral budding. J Virol **73**:2921-9.

26. **Henning, J., J. Morton, T. Hla, and J. Meers.** 2008. Mortality rates adjusted for unobserved deaths and associations with Newcastle disease virus serology among unvaccinated village chickens in Myanmar. Prev Vet Med **85**:241-52.

27. **Henrickson, K. J.** 2003. Parainfluenza viruses. Clin Microbiol Rev **16**:242-64.

28. **Huang, M., J. M. Orenstein, M. A. Martin, and E. O. Freed.** 1995. p6Gag is required for particle production from full-length human immunodeficiency virus type 1 molecular clones expressing protease. J Virol **69**:6810-8.

29. **Iorio, R. M., and P. J. Mahon.** 2008. Paramyxoviruses: different receptors - different mechanisms of fusion. Trends Microbiol **16**:135-7.

30. **Irie, T., and R. N. Harty.** 2005. L-domain flanking sequences are important for host interactions and efficient budding of vesicular stomatitis virus recombinants. J Virol **79**:12617-22.

31. **Irie, T., M. Inoue, and T. Sakaguchi.** 2010. Significance of the YLDL motif in the M protein and Alix/AIP1 for Sendai virus budding in the context of virus infection. Virology **405**:334-41.

32. **Irie, T., J. M. Licata, and R. N. Harty.** 2005. Functional characterization of Ebola virus L-domains using VSV recombinants. Virology **336**:291-8.

33. **Irie, T., J. M. Licata, J. P. McGettigan, M. J. Schnell, and R. N. Harty.** 2004. Budding of PPxY-containing rhabdoviruses is not dependent on host proteins TSG101 and VPS4A. J Virol **78**:2657-65.

34. **Irie, T., N. Nagata, T. Yoshida, and T. Sakaguchi.** 2008. Recruitment of Alix/AIP1 to the plasma membrane by Sendai virus C protein facilitates budding of virus-like particles. Virology **371**:108-20.

35. **Irie, T., Y. Shimazu, T. Yoshida, and T. Sakaguchi.** 2007. The YLDL sequence within Sendai virus M protein is critical for budding of virus-like particles and interacts with Alix/AIP1 independently of C protein. J Virol **81**:2263-73.

36. **Jayakar, H. R., K. G. Murti, and M. A. Whitt.** 2000. Mutations in the PPPY motif of vesicular stomatitis virus matrix protein reduce virus budding by inhibiting a late step in virion release. J Virol **74**:9818-27.

37. **Justice, P. A., W. Sun, Y. Li, Z. Ye, P. R. Grigera, and R. R. Wagner.** 1995. Membrane vesiculation function and exocytosis of wild-type and mutant matrix proteins of vesicular stomatitis virus. J Virol **69**:3156-60.

38. **Katzmann, D. J., M. Babst, and S. D. Emr.** 2001. Ubiquitin-dependent sorting into the multivesicular body pathway requires the function of a conserved endosomal protein sorting complex, ESCRT-I. Cell **106**:145-55.

39. **Kingsbury, D. W.** 1991. The Paramyxoviruses. Plenum Press, New York.

40. **Lamb, R. A., and P. W. Choppin.** 1976. Synthesis of influenza virus proteins in infected cells: translation of viral polypeptides, including three P polypeptides, from RNA produced by primary transcription. Virology **74**:504-19.

41. **Lee, M. S., R. E. Walker, and P. M. Mendelman.** 2005. Medical burden of respiratory syncytial virus and parainfluenza virus type 3 infection among US children. Implications for design of vaccine trials. Hum Vaccin **1**:6-11.

42. **Li, M., P. T. Schmitt, Z. Li, T. S. McCrory, B. He, and A. P. Schmitt.** 2009. Mumps virus matrix, fusion, and nucleocapsid proteins cooperate for efficient production of virus-like particles. J Virol **83**:7261-72.

43. **Licata, J. M., R. F. Johnson, Z. Han, and R. N. Harty.** 2004. Contribution of ebola virus glycoprotein, nucleoprotein, and VP24 to budding of VP40 virus-like particles. J Virol **78**:7344-51.

44. **Licata, J. M., M. Simpson-Holley, N. T. Wright, Z. Han, J. Paragas, and R. N. Harty.** 2003. Overlapping motifs (PTAP and PPEY) within the Ebola virus VP40 protein function independently as late budding domains: involvement of host proteins TSG101 and VPS-4. J Virol **77**:1812-9.

45. **Liu, Y., L. Cocka, A. Okumura, Y. A. Zhang, J. O. Sunyer, and R. N. Harty.** 2010. Conserved motifs within Ebola and Marburg virus VP40 proteins are important for stability, localization, and subsequent budding of virus-like particles. J Virol **84**:2294-303.

46. **Madhi, S. A., C. Cutland, Y. Zhu, J. G. Hackell, F. Newman, N. Blackburn, B. R. Murphy, R. B. Belshe, R. A. Karron, A. M. Deatly, W. C. Gruber, D. I. Bernstein, and P. F. Wright.** 2006. Transmissibility, infectivity and immunogenicity of a live human parainfluenza type 3 virus vaccine (HPIV3cp45) among susceptible infants and toddlers. Vaccine **24**:2432-9.

47. **Mao, H., C. S. Thakur, S. Chattopadhyay, R. H. Silverman, A. Gudkov, and A. K. Banerjee.** 2008. Inhibition of human parainfluenza virus type 3 infection by novel small molecules. Antiviral Res **77**:83-94.

48. **Marcos, M. A., M. Esperatti, and A. Torres.** 2009. Viral pneumonia. Curr Opin Infect Dis **22**:143-7.

49. **Martin-Serrano, J., D. Perez-Caballero, and P. D. Bieniasz.** 2004. Context-dependent effects of L domains and ubiquitination on viral budding. J Virol **78**:5554-63.

50. **Martin-Serrano, J., T. Zang, and P. D. Bieniasz.** 2001. HIV-1 and Ebola virus encode small peptide motifs that recruit Tsg101 to sites of particle assembly to facilitate egress. Nat Med **7**:1313-9.

51. **Matsumoto, T.** 1982. Assembly of paramyxoviruses. Microbiol Immunol **26**:285-320.

52. **Mottet, G., A. Muhlemann, C. Tapparel, F. Hoffmann, and L. Roux.** 1996. A Sendai virus vector leading to the efficient expression of mutant M proteins interfering with virus particle budding. Virology **221**:159-71.

53. **Neumann, G., H. Ebihara, A. Takada, T. Noda, D. Kobasa, L. D. Jasenosky, S. Watanabe, J. H. Kim, H. Feldmann, and Y. Kawaoka.** 2005. Ebola virus VP40 late domains are not essential for viral replication in cell culture. J Virol **79**:10300-7.

54. **Nickerson, D. P., M. R. Russell, and G. Odorizzi.** 2007. A concentric circle model of multivesicular body cargo sorting. EMBO Rep **8**:644-50.

55. **Noda, T., H. Sagara, E. Suzuki, A. Takada, H. Kida, and Y. Kawaoka.** 2002. Ebola virus VP40 drives the formation of virus-like filamentous particles along with GP. J Virol **76**:4855-65.

56. **Parent, L. J., R. P. Bennett, R. C. Craven, T. D. Nelle, N. K. Krishna, J. B. Bowzard, C. B. Wilson, B. A. Puffer, R. C. Montelaro, and J. W. Wills.** 1995. Positionally independent and exchangeable late budding functions of the Rous sarcoma virus and human immunodeficiency virus Gag proteins. J Virol **69**:5455-60.

57. **Patch, J. R., Z. Han, S. E. McCarthy, L. Yan, L. F. Wang, R. N. Harty, and C. C. Broder.** 2008. The YPLGVG sequence of the Nipah virus matrix protein is required for budding. Virol J **5**:137.

58. **Patnaik, A., V. Chau, F. Li, R. C. Montelaro, and J. W. Wills.** 2002. Budding of equine infectious anemia virus is insensitive to proteasome inhibitors. J Virol **76**:2641-7.

59. **Raiborg, C., and H. Stenmark.** 2009. The ESCRT machinery in endosomal sorting of ubiquitylated membrane proteins. Nature **458**:445-52.

60. **Rossman, J.S., Jing, X., Leser, G.P., and R. A. Lamb.** 2010. Influenza virus M2 protein mediates ESCRT-independent membrane scission. Cell **142**:902-13.

61. **Sakaguchi, T., A. Kato, F. Sugahara, Y. Shimazu, M. Inoue, K. Kiyotani, Y. Nagai, and T. Yoshida.** 2005. AIP1/Alix is a binding partner of Sendai virus C protein and facilitates virus budding. J Virol 79:8933-41.

62. **Salditt, A., S. Koethe, C. Pohl, H. Harms, L. Kolesnikova, S. Becker, and S. Schneider-Schaulies.** 2010. Measles virus M protein-driven particle production does not involve the endosomal sorting complex required for transport (ESCRT) system. J Gen Virol **91**:1464-72.

63. **Schmitt, A. P., B. He, and R. A. Lamb.** 1999. Involvement of the cytoplasmic domain of the hemagglutinin-neuraminidase protein in assembly of the paramyxovirus simian virus 5. J Virol **73**:8703-12.

64. **Schmitt, A. P., G. P. Leser, E. Morita, W. I. Sundquist, and R. A. Lamb.** 2005. Evidence for a new viral late-domain core sequence, FPIV, necessary for budding of a paramyxovirus. J Virol **79**:2988-97.

65. **Smith, C. B., R. H. Purcell, J. A. Bellanti, and R. M. Chanock.** 1966. Protective effect of antibody to parainfluenza type 1 virus. N Engl J Med **275**:1145-52.

66. **Spidel, J. L., R. C. Craven, C. B. Wilson, A. Patnaik, H. Wang, L. M. Mansky, and J. W. Wills.** 2004. Lysines close to the Rous sarcoma virus late domain critical for budding. J Virol **78**:10606-16.

67. **Spriggs, M. K., and P. L. Collins.** 1986. Human parainfluenza virus type 3: messenger RNAs, polypeptide coding assignments, intergenic sequences, and genetic map. J Virol **59**:646-54.

68. **Tanaka, Y., J. Kato, M. Kohara, and M. S. Galinski.** 2006. Antiviral effects of glycosylation and glucose trimming inhibitors on human parainfluenza virus type 3. Antiviral Res **72**:1-9.

69. **Taylor, G. M., P. I. Hanson, and M. Kielian.** 2007. Ubiquitin depletion and dominant-negative VPS4 inhibit rhabdovirus budding without affecting alphavirus budding. J Virol **81**:13631-9.

70. **Timmins, J., G. Schoehn, S. Ricard-Blum, S. Scianimanico, T. Vernet, R. W. Ruigrok, and W. Weissenhorn.** 2003. Ebola virus matrix protein VP40 interaction with human cellular factors Tsg101 and Nedd4. J Mol Biol **326**:493-502.

71. **Timmins, J., S. Scianimanico, G. Schoehn, and W. Weissenhorn.** 2001. Vesicular release of ebola virus matrix protein VP40. Virology **283**:1-6.

72. **Urata, S., T. Noda, Y. Kawaoka, S. Morikawa, H. Yokosawa, and J. Yasuda.** 2007. Interaction of Tsg101 with Marburg virus VP40 depends on the PPPY motif, but not the PT/SAP motif as in the case of Ebola virus, and Tsg101 plays a critical role in the budding of Marburg virus-like particles induced by VP40, NP, and GP. J Virol **81**:4895-9.

73. **Urata, S., T. Noda, Y. Kawaoka, H. Yokosawa, and J. Yasuda.** 2006. Cellular factors required for Lassa virus budding. J Virol **80**:4191-5.

74. **Urata, S., and J. Yasuda.** 2010. Regulation of Marburg virus (MARV) budding by Nedd4.1: a different WW domain of Nedd4.1 is critical for binding to MARV and Ebola virus VP40. J Gen Virol **91**:228-34.

75. **Utley, T. J., N. A. Ducharme, V. Varthakavi, B. E. Shepherd, P. J. Santangelo, M. E. Lindquist, J. R. Goldenring, and J. E. Crowe, Jr.** 2008. Respiratory syncytial virus uses a Vps4-independent budding mechanism controlled by Rab11-FIP2. Proc Natl Acad Sci U S A **105**:10209-14.

76. **VerPlank, L., F. Bouamr, T. J. LaGrassa, B. Agresta, A. Kikonyogo, J. Leis, and C. A. Carter.** 2001. Tsg101, a homologue of ubiquitin-conjugating (E2) enzymes, binds the L domain in HIV type 1 Pr55(Gag). Proc Natl Acad Sci U S A **98**:7724-9.

77. **Watanabe, H., Y. Tanaka, Y. Shimazu, F. Sugahara, M. Kuwayama, A. Hiramatsu, K. Kiyotani, T. Yoshida, and T. Sakaguchi.** 2005. Cell-specific inhibition of paramyxovirus maturation by proteasome inhibitors. Microbiol Immunol **49**:835-44.

75. **Weinberg, G. A., C. B. Hall, M. K. Iwane, K. A. Poehling, K. M. Edwards, M. R. Griffin, M. A. Staat, A. T. Curns, D. D. Erdman, and P. G. Szilagyi.** 2009. Parainfluenza virus infection of young children: estimates of the population-based burden of hospitalization. J Pediatr **154**:694-9.

79. **Welsch, S., B. Muller, and H. G. Krausslich.** 2007. More than one door - Budding of enveloped viruses through cellular membranes. FEBS Lett **581**:2089-97.

80. **Wills, J. W., C. E. Cameron, C. B. Wilson, Y. Xiang, R. P. Bennett, and J. Leis.** 1994. An assembly domain of the Rous sarcoma virus Gag protein required late in budding. J Virol **68**:6605-18.

81. **Wirblich, C., G. S. Tan, A. Papaneri, P. J. Godlewski, J. M. Orenstein, R. N. Harty, and M. J. Schnell.** 2008. PPEY motif within the rabies virus (RV) matrix protein is essential for efficient virion release and RV pathogenicity. J Virol **82**:9730-8.

82. **Wolfson, L. J., F. Gasse, S. P. Lee-Martin, P. Lydon, A. Magan, A. Tibouti, B. Johns, R. Hutubessy, P. Salama, and J. M. Okwo-Bele.** 2008. Estimating the costs of achieving the WHO-UNICEF Global Immunization Vision and Strategy, 2006-2015. Bull World Health Organ **86**:27-39.

83. **Wolfson, L. J., P. M. Strebel, M. Gacic-Dobo, E. J. Hoekstra, J. W. McFarland, and B. S. Hersh.** 2007. Has the 2005 measles mortality reduction goal been achieved? A natural history modelling study. Lancet **369**:191-200.

84. **Yamayoshi, S., and Y. Kawaoka.** 2007. Mapping of a region of Ebola virus VP40 that is important in the production of virus-like particles. J Infect Dis **196** Suppl 2:S291-5.

85. **Yasuda, J., Nakao, M., Kawaoka, Y., and H. Shida.** 2003. Nedd4 regulates egress of Ebola virus-like particles from host cells. J Virol. **18**:9987-92.

86. **Zhadina, M., M. O. McClure, M. C. Johnson, and P. D. Bieniasz.** 2007. Ubiquitin-dependent virus particle budding without viral protein ubiquitination. Proc Natl Acad Sci U S A **104**:20031-6.

APPENDIX A

ALIGNMENT OF MATRIX PROTEINS FROM MEMBERS OF THE SUBFAMILY *PARAMYXOVIRINAE*

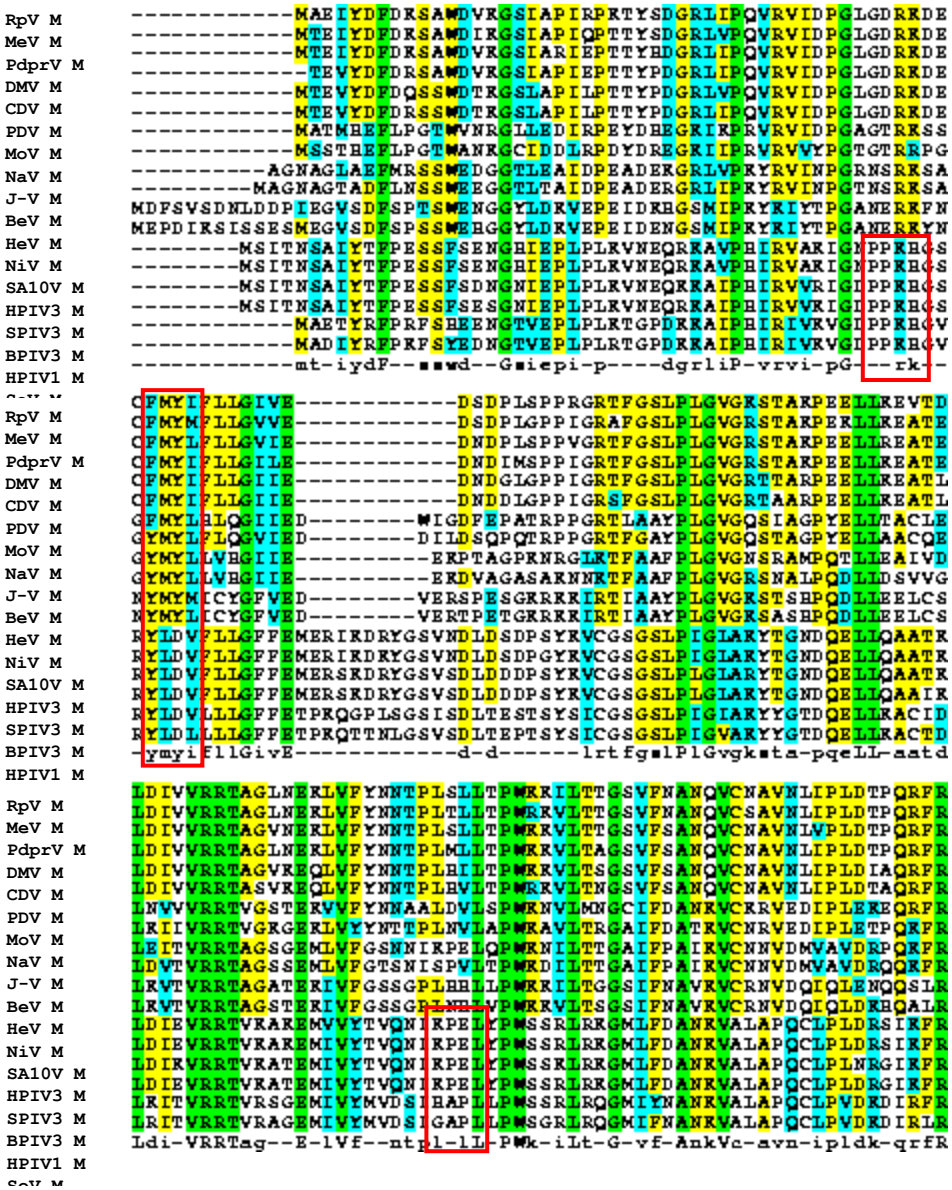
RpV M
MeV M
PdprV M
DMV M
CDV M
PDV M
MoV M
NaV M
J-V M
BeV M
HeV M
NiV M
SA10V M
HPIV3 M
SPIV3 M
BPIV3 M
HPIV1 M

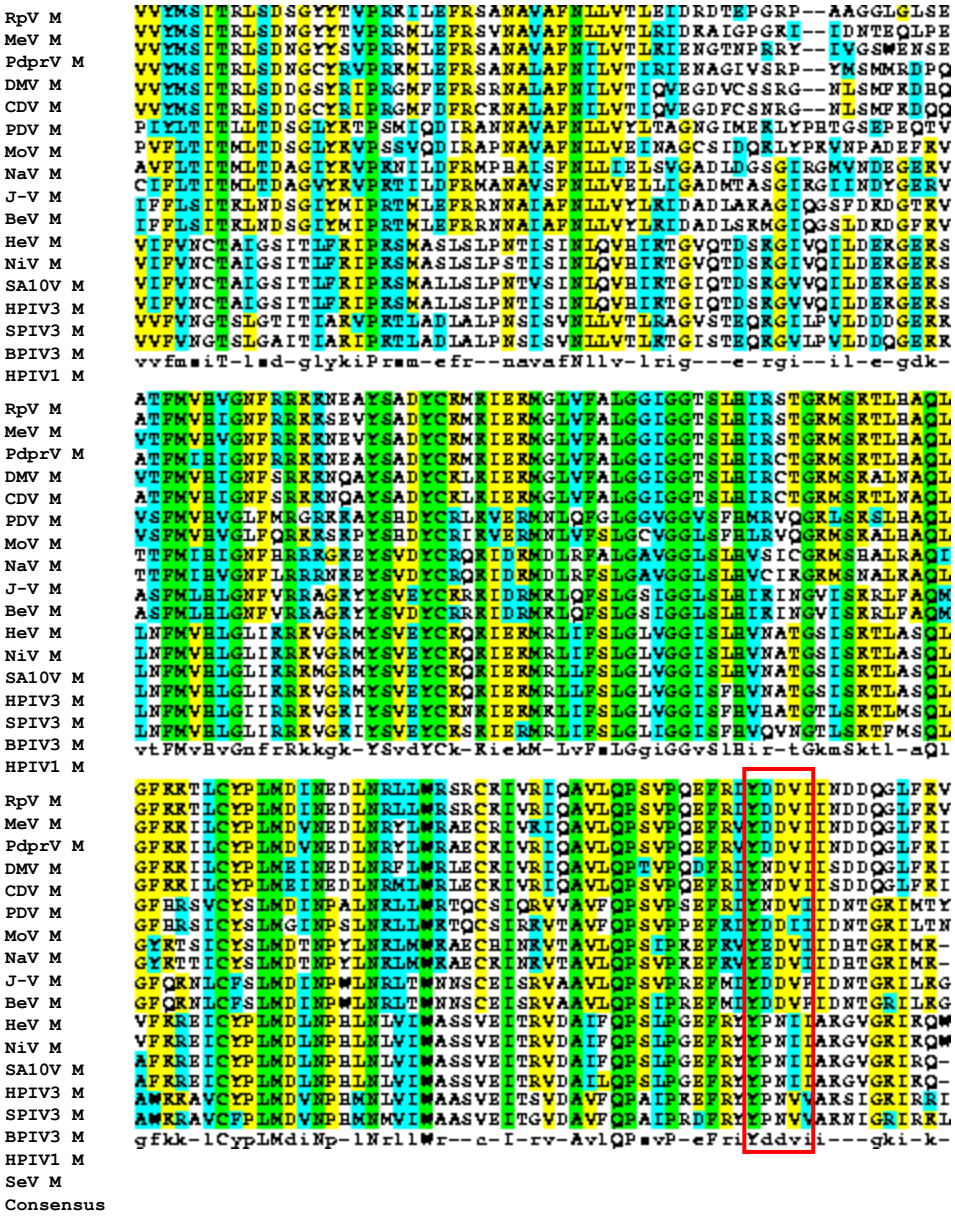

Fig. 1. Matrix protein ClustalW alignment of eighteen viruses within the subfamily *Paramyxovirinae*. Each of the four candidate L domains of HPIV3 along with the aligned sequences from related viruses is boxed in red. The abbreviations are for: Rinderpest virus (RPV), measles virus (MeV), pestes-des-petits-ruminiants virus (PdprV), dolphin morbillivirus (DMV), canine distemper virus (CDV), phocine distemper virus (PDV), Mossman virus (MoV), Nariva virus (NaV), J Virus (J-V), Beilong virus (BeV), Hendra virus (HeV), Nipah virus (NiV), simian agent 10 virus (SA10V), swine parainfluenza virus 3 (SPIV3), bovine parainfluenza virus 3 (BPIV3), human parainfluenza virus 1 (HPIV1), and Sendai virus (SeV).

APPENDIX B

PHENOGRAM OF MATRIX PROTEINS FROM MEMBERS OF THE SUBFAMILY *PARAMYXOVIRINAE*

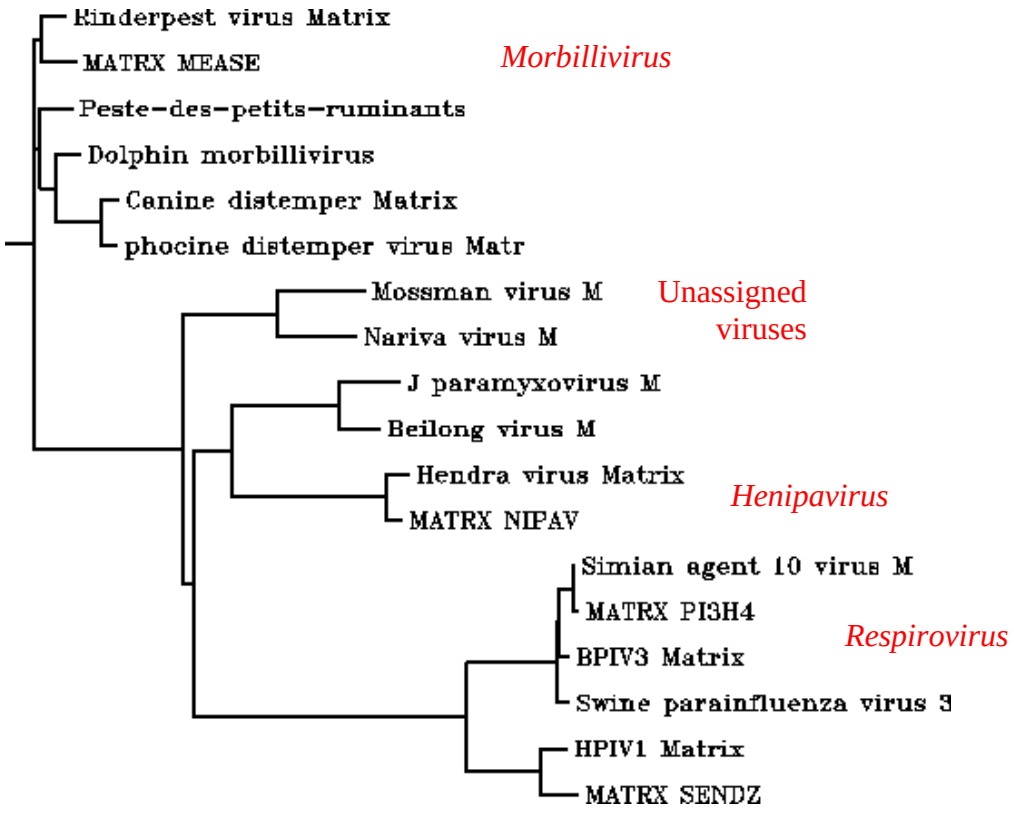

Fig. 2. Rooted phylogenetic tree of eighteen members of the subfamily *Paramyxovirinae* based on Biology Workbench's ClustalW-generated M protein alignments. Each genus is labeled in red; the Mossman, Nariva, Beilong, and J viruses have yet to be assigned to a genus. The alignment excludes positions with gaps and corrects for multiple substitutions. Branch lengths were automatically rescaled with intermediate ancestral nodes.